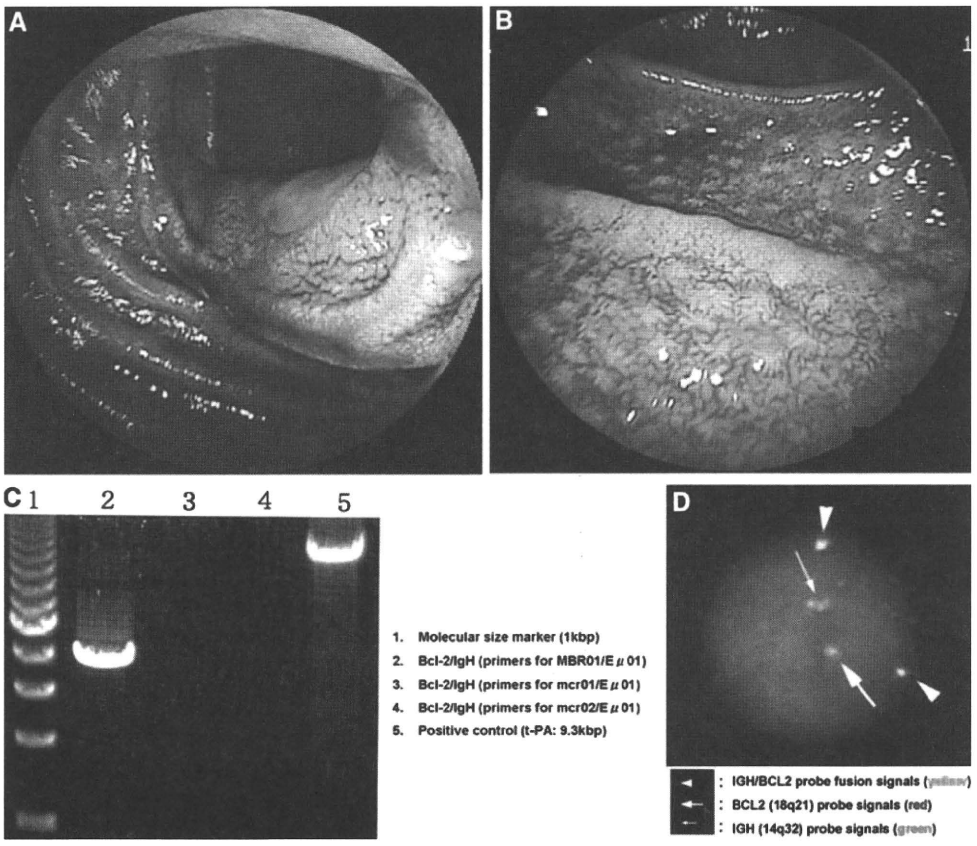

Fig. 7 Endoscopic findings of GI-FL, **c** polymerase chain reaction (PCR) analysis of GI-FL, and **d** fluorescence in situ hybridization (FISH) analysis of GI-FL in a 47-year-old man. DBE revealed a submucosal tumor-like lesion with ulceration in the middle portion of the small intestine (**a**). There were small whitish granular lesions on the oral side of the ulcer (**b**). PCR analysis. *IgH/BCL2* rearrangement was detected with probes for major break region (*MBR*; **c**). FISH analysis. *t*(11;14)(q13;q32) was demonstrated by the yellow fusion signals in an abnormal nucleus (**d**). *mcr*, Minor cluster region

Table 6 Histologic grade of GI-FL

Histologic grade	*n* (%)
Grade 1	157 (84.4)
Grade 2	21 (11.3)
Grade 3	8 (4.3)
Grade 3a	3 (1.6)
Grade 3b	1 (0.5)
Details unknown	4 (2.2)

Table 7 Immunophenotype of GI-FL

	n (%)
Surface marker	
CD10 (+), Bcl-2 (+)	155 (68.9)
CD10 (+), Bcl-2 (−)	3 (1.3)
CD10 (−), Bcl-2 (+)	7 (3.1)
CD10 (−), Bcl-2 (−)	3 (1.3)
CD10 (?), Bcl-2 (+)	51 (22.7)
CD10 (?), Bcl-2 (−)	6 (2.7)
Surface immunoglobulin	
IgM	14 (50.0)
IgD	4 (15.4)
IgA	4 (15.4)
IgG	2 (7.7)
Not detected	3 (11.5)

of gastric FL [37] and 2 cases of FL of the small intestine [32]. In all of these cases, the primary lesion formed a mass lesion. It is noteworthy that small mediastinal lymph node dissemination was detected with FDG-PET in one gastric FL case (Fig. 6c, arrowhead) [37]. In this case, the disseminated lesion above the diaphragm could not be detected with CT, which was performed before the FDG-PET examination. In another case of duodenal FL [24], 18F-FDG accumulated in the mesenteric lymph nodes, whereas there was no obvious uptake in the primary site. Therefore, this modality may not be useful for evaluating the spread of the primary lesion, as Hoffman et al. [44] and Higuchi et al. [32] demonstrated, but the modality is useful for evaluating lymph node dissemination.

Prognosis in patients with gastrointestinal follicular lymphoma

Prognosis of GI-FL

The long-term clinical outcome of GI-FL remains unclear because there has been no analysis of a large population-based registry of survival for patients with GI-FL. In 2 case

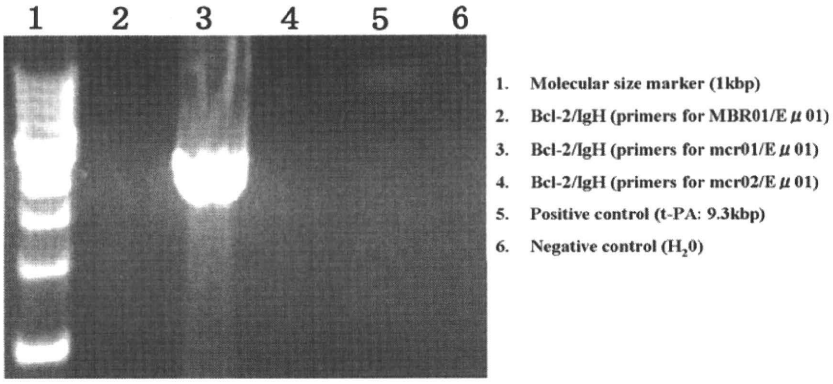

Fig. 8 PCR analysis in an 81-year-old woman with GI-FL. Primers for MBR failed to detect *t*(14;18)(q32;q21) (*lane 2*), and PCR products using primers for mcr were observed in *lane 3*

Table 8 Genetic features of GI-FL

	n (%)
Southern blotting	
Positive (MBR)	1 (20.0)
Positive (mcr)	1 (20.0)
Positive (break point unknown)	1 (20.0)
Negative (MBR and mcr)	2 (40.0)
Polymerase chain reaction	
Positive (MBR)	23 (46.9)
Positive (mcr)	1 (2.0)
Positive (break point unknown)	4 (8.2)
Negative (MBR)	21 (42.9)
Fluorescence in situ hybridization	
Positive	18 (72.0)
Negative	7 (28.0)

MBR major breakpoint region, *mcr* minor cluster region

series on long-term outcomes of patients with GI-FL, relapse-free median time or median relapse-free survival was similar to that for nodal FL [12, 15]. Shia et al. [15] reported a median relapse-free survival of 63 months in 25 GI-FL patients. Damaj et al. [12] reported a median time to progression of 37.5 months in 7 patients without any treatment and a median time to recurrence of the disease of 31 months in 18 patients with treatment.

On the other hand, based on all available data reported previously, GI-FL seems to have a better prognosis than nodal FL. There are only five reported cases in which the patients died of GI-FL, and, among 249 GI-FL patients, 3 patients died of another disease [12, 20, 22, 54]. In addition, the median relapse-free survival was 98 months in 96 patients with GI-FL (Fig. 9a), which appears to be a more favorable outcome compared with that of nodal FL.

In GI-FL, the frequency of grade 1 lymphoma is much higher compared with that in nodal FL (see "Histologic grading"), and most GI-FL presents as a localized disease at the time of diagnosis, while most nodal FL involves multiple sites when staging procedures are performed (see "Clinical stage"). These features may indicate that GI-FL is a distinct entity from nodal FL, and is slower to progress.

There may be other reasons for the better prognosis of GI-FL compared with that of nodal FL. When lymphoma cells infiltrate not only the GI tract but also extraintestinal sites, e.g., peripheral or mediastinal lymph nodes, liver or spleen, most such cases, especially those with massive extraintestinal lesions, are excluded from primary GI-FL [11, 12, 15–17] because of the inability to distinguish between primary GI-FL with extraintestinal invasion and secondary GI-FL as a result of dissemination from another site (see "Definition of primary GI lymphoma"). Second, there are only a few GI-FL patients with a long-term follow up, because of its rarity. The median follow-up duration of the reported cases of GI-FL is only 24.5 months, while the median follow up was more than 50 months in most studies of the long-term clinical outcome of nodal FL [103–105].

Grade 1 GI-FL tends to have a better relapse-free survival than grade 2 GI-FL, but the prognosis for grade 3 lymphoma is unclear because of its rarity. Relapse-free survival of grade 1, grade 2, and grade 3 is 61.6% at 180 months ($n = 48$), 41.7% at 112 months ($n = 13$), and 100% at 108 months ($n = 3$), respectively (Fig. 9b). The difference in overall survival between each grade is also unknown, as only 5 patients died of GI-FL and 3 died of other diseases, based on the data in the available literature [12, 20, 22, 54].

To compare the prognosis between localized GI-FLs (i.e., stage I or II) and systemic ones (i.e., stage III or IV) is difficult, because only 13 of 193 GI-FL patients (6.7%) with available clinical stage data had a systemic disease.

Recurrence after achieving complete remission in GI-FL

Of 249 patients with GI-FL, 106 achieved complete remission with various therapies (see "Gastrointestinal follicular lymphoma treatment"). Of those, FL relapsed in 16 cases from 1 to 98 months after achieving of complete remission [12, 15–17, 47]. Details of relapsed cases are summarized in Table 9. Median time to recurrence was

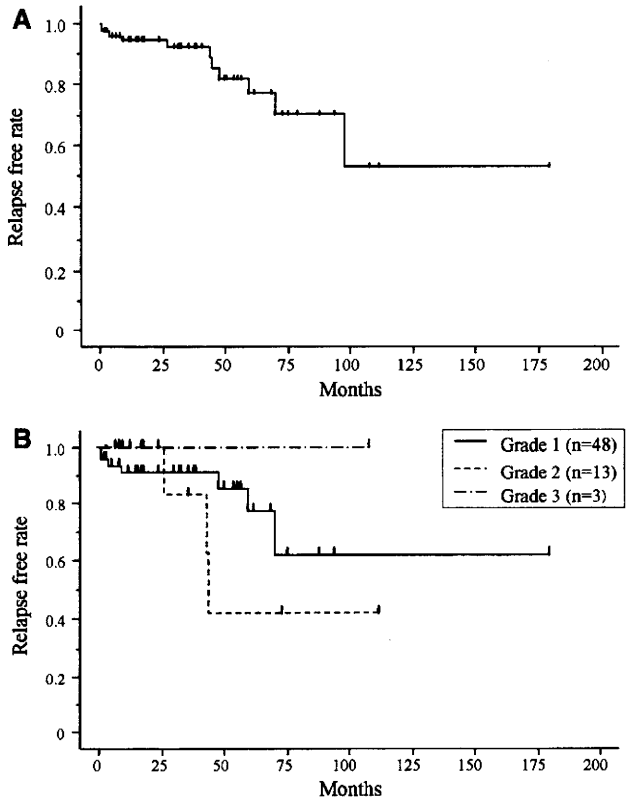

Fig. 9 **a** Kaplan–Meier plot of relapse-free survival after achieving complete remission in patients with GI-FL. **b** Relapse-free survival according to histologic grade. Relapse-free survival of grade 1, grade 2, and grade 3 was 61.6% at 180 months ($n = 48$), 41.7% at 112 months ($n = 13$), and 100% at 108 months ($n = 3$), respectively

44.5 months. Initial treatments to induce remission were surgery (4 cases), radiation (1 case), chemotherapy (4 cases), radiation plus chemotherapy (2 cases), surgery plus chemotherapy (4 cases), and radiation plus surgery following chemotherapy (1 case). It is noteworthy that FL relapsed outside the GI tract, including in extraabdominal lymph nodes, the spleen, and tonsils, in about 50% of the recurrent cases [15–17]. Therefore, not only evaluation of the GI tract using endoscopy and abdominal CT scan but also whole-body evaluation, including gallium scintigram or FDG-PET, should be performed for follow-up studies after the achieving of complete remission. To screen for extraabdominal relapse, FDG-PET rather than gallium scintigraphy is recommended because of its sensitivity [100] (see "Recent advances in gastrointestinal follicular lymphoma staging").

Gastrointestinal follicular lymphoma treatment

Management of GI-FL is controversial, mainly because of its rarity. Damaj et al. [12] reported that there was no significant difference in the prognosis between patients without treatment and those with treatment, as in nodal FL

Table 9 Recurrence after achieving complete remission in GI-FL

	n
Number of cases with recurrence	16
Sex	
Male/female/unknown	5/5/6
Median time to recurrence (months)	44.5[a]
Range (months)	1–98[a]
Clinical stage	
I/II/IV/unknown	6/3/1/6
Initial treatments	
Surgery	4
Radiation	1
Chemotherapy	4
Radiation + chemotherapy	2
Surgery + chemotherapy	4
Surgery + radiation + chemotherapy	1
Recurrent site	
Local recurrence	1
Locoregional recurrence	6
Outside the GI tract	7[b]
Unknown	2

[a] 6 cases in which the duration of remission was not described were excluded

[b] Recurrent sites were submandibular lymph nodes (1 case), axillary and inguinal lymph nodes (1 case), colon and spleen (1 case), tonsil (1 case), and unknown (3 cases)

[106–108]. Therefore, a "watch and wait policy" has been adopted in some asymptomatic patients with GI-FL [13, 15, 17, 18, 20, 23, 54, 55]. In other patients, surgery, radiotherapy, chemotherapy, monoclonal antibody therapy, or a combination of these therapies is performed. In addition, antibiotic therapy has been tried in several patients with GI-FL [7, 17–19, 24, 25, 34, 50], based on the established efficacy of antibiotics in patients with other indolent GI lymphomas, such as gastric MALT lymphoma or immunoproliferative small intestinal disease (IPSID).

GI-FL treatments and responses are summarized in Table 10.

Conventional therapies

Patients with GI-FL have been treated with surgery, radiotherapy, chemotherapy, or a combination of these therapies. To compare the effect of each therapy with another is difficult, however, because the number of patients receiving each type of treatment is very small and the background of the cases, including clinical stage and duration of follow up, varies. In general, a complete response was achieved in most patients regardless of treatment modality, reflecting the indolent nature of GI-FL

Table 10 Therapeutic modalities for GI-FL

	n	Response to the therapies ($n = 159$)				
		CR (recurrence)	PR	NC	PD	unknown
Surgery	36	28 (4)	2	0	0	6
Radiation	6	6 (1)	0	0	0	0
Chemotherapy without rituximab	44	22 (4)	9	2	1	10
Chemotherapy + radiation	8	4 (2)	1	1	0	2
Surgery + chemotherapy	24	20 (4)	2	0	0	2
Surgery + radiation	1	1 (0)	0	0	0	0
Surgery + radiation + chemotherapy	1	1 (1)	0	0	0	0
Rituximab monotherapy	8	6 (0)	2	0	0	0
Chemotherapy + rituximab	19	15 (0)	4	0	0	0
Surgery + chemotherapy + rituximab	1	1 (0)	0	0	0	0
Antibiotic therapy	15	2 (0)	1	9	2	1
Observation	48	–	–	–	–	–
Total	211	106 (16)	21	12	3	21

CR complete response, *PR* partial response, *NC* no change, *PD* progressive disease

(Table 10) (see "Prognosis in patients with gastrointestinal follicular lymphoma").

Chemotherapy for GI-FL is performed based on the therapeutic regimens of nodal FL, especially in patients with systemic disease or widespread GI tract involvement.

Rituximab-containing regimen

After the introduction of therapies using the monoclonal antibody against CD20, rituximab, several randomized studies demonstrated that this therapeutic modality, combined with conventional therapies, improved not only the complete response rate and the duration of the response but also the overall survival rate of nodal FL [109–111]. In addition, in GI-FL, immunotherapy using rituximab with or without chemotherapy has been performed [7, 13, 16–18, 20, 24, 28, 41, 42, 56], although the efficacy of therapy including rituximab has not been compared with that of conventional therapy alone. There seems to be no difference in the response of GI-FL between therapeutic regimens containing rituximab and conventional therapy at present, which may be due to the disease rarity and the favorable nature of the disease (Table 10).

Antibiotic therapy

Growing evidence indicates that some subtypes of marginal zone lymphomas are associated with chronic antigen stimulation by microbial pathogens and that therapy with antibiotics is effective in marginal zone lymphoma of MALT type, including gastric MALT lymphoma and IPSID.

Several studies have revealed a close association of infection with *H. pylori* and gastric MALT lymphoma [112–115], and the eradication of *H. pylori* infection results in lymphoma remission in patients with low-grade MALT lymphoma localized in the stomach [116–122].

IPSID, which is also called "Mediterranean lymphoma" or "alpha heavy chain disease" [123], is a variant of MALT lymphoma in the small intestine. Early-stage IPSID responds to antibiotics such as tetracycline, ampicillin, or metronidazole [124]. Recently Lecuit et al. [125] have reported that IPSID is associated with *Campylobacter jejuni*.

Also in GI-FL, some patients were treated with antibiotics using an *H. pylori* eradication regimen, because *H. pylori* was detected in the stomach or a diagnosis of MALT lymphoma was made at first. Most GI-FL lesions, however, were unchanged or progressed despite the administration of antibiotic agents [17, 18, 24, 25, 50]. The fact that antibiotic therapy is ineffective for most patients with GI-FL may indicate that the neoplastic follicles of GI-FL are not composed of antigen-driven cells, different from MALT lymphoma [126].

In several patients with GI-FL, however, regression of GI-FL was noted after antibiotic treatment [14, 19, 34]. Toyoda et al. reported a case of duodenal FL that regressed 12 months after eradication of *H. pylori* although the immunophenotype of the tumor cells was CD10- and bcl-2+, which is characteristic of MALT lymphoma rather than FL [19]. Nakamura et al. [14] described a patient who showed regression of GI-FL at 15 months after antibiotic treatment, and Nomura et al. [34] reported that duodenal FL regressed at 12 months after antibiotic therapy. These cases may suggest that tumor cell growth depends on stimulation with antigens originating from the gut lumen via B-cell receptors on the tumor cells in some cases of

GI-FL, as Bende et al. [45] and Takata et al. [63] have speculated.

Conclusion

Although GI-FL is generally considered to be a rare entity, the number of reported cases of GI-FL is increasing. A consensus regarding the management of this disorder, however, has not yet been established. Irrespective of the specific therapy, the overall survival of GI-FL appears to be good. Little is known about long-term clinical outcome of GI-FL, especially since treatment with rituximab was introduced. Therefore, further studies are necessary to evaluate how rituximab changes the clinical outcome of GI-FL.

Accurate evaluation of the distribution of the disease, however, is necessary for deciding on the treatment modality. WCE and DBE, which provide detailed information about the mucosa of the whole small intestine, are useful for localizing GI-FL because of the potential multifocal involvement of the GI tract in many cases. GI-FL tends to be localized in the GI tract and regional lymph nodes at diagnosis, whereas extraabdominal relapse is observed in about 50% of recurrent cases. Accordingly, endoscopic examination throughout the entire GI tract and whole-body evaluation with FDG-PET is necessary for staging and follow-up studies.

References

1. Anderson JR, Armitage JO, Weisenburger DD. Epidemiology of the non-Hodgkin's lymphomas: distribution of the major subtypes differ by geographic locations. Non-Hodgkin's Lymphoma Classification Project. Ann Oncol. 1998;9:717–20.
2. Goodlad JR, MacPherson S, Jackson R, Batstone P, White J. Extranodal follicular lymphoma: a clinicopathological and genetic analysis of 15 cases arising at non-cutaneous extranodal sites. Histopathology. 2004;44:268–76.
3. d'Amore F, Christensen BE, Brincker H, Pedersen NT, Thorling K, Hastrup J, et al. Clinicopathological features and prognostic factors in extranodal non-Hodgkin lymphomas. Danish LYFO Study Group. Eur J Cancer. 1991;27:1201–8.
4. Cirillo M, Federico M, Curci G, Tamborrino E, Piccinini L, Silingardi V. Primary gastrointestinal lymphoma: a clinicopathological study of 58 cases. Haematologica. 1992;77:156–61.
5. Morton JE, Leyland MJ, Vaughan Hudson G, Vaughan Hudson B, Anderson L, Bennett MH, et al. Primary gastrointestinal non-Hodgkin's lymphoma: a review of 175 British National Lymphoma Investigation cases. Br J Cancer. 1993;67:776–82.
6. Koh PK, Horsman JM, Radstone CR, Hancock H, Goepel JR, Hancock BW. Localised extranodal non-Hodgkin's lymphoma of the gastrointestinal tract: Sheffield Lymphoma Group experience (1989–1998). Int J Oncol. 2001;18:743–8.
7. Nakamura S, Matsumoto T, Iida M, Yao T, Tsuneyoshi M. Primary gastrointestinal lymphoma in Japan: a clinicopathologic analysis of 455 patients with special reference to its time trends. Cancer. 2003;97:2462–73.
8. Yoshino T, Miyake K, Ichimura K, Mannami T, Ohara N, Hamazaki S, et al. Increased incidence of follicular lymphoma in the duodenum. Am J Surg Pathol. 2000;24:688–93.
9. Lewin KJ, Ranchod M, Dorfman R. Lymphomas of the gastrointestinal tract: a study of 117 cases presenting with gastrointestinal disease. Cancer. 1978;42:693–707.
10. Filippa DA, Lieberman PH, Weingrad DN, Decosse JJ, Bretsky SS. Primary lymphomas of the gastrointestinal tract: analysis of prognostic factors with emphasis on histological type. Am J Surg Pathol. 1983;7:363–72.
11. LeBrun DP, Ngan BY, Weiss LM, Huie P, Warnke RA, Cleary ML. Follicular lymphomas of the gastrointestinal tract. Pathologic features in 31 cases and bcl-2 oncogenic protein expression. Am J Pathol. 1992;140:1327–35.
12. Damaj G, Verkarre V, Delmer A, Solal-Celigny P, Yakoub-Agha I, Cellier C, et al. Primary follicular lymphoma of the gastrointestinal tract: a study of 25 cases and a literature review. Ann Oncol. 2003;14:623–9.
13. Kodama M, Kitadai Y, Shishido T, Shimamoto M, Fukumoto A, Masuda H, et al. Primary follicular lymphoma of the gastrointestinal tract: a retrospective case series. Endoscopy. 2008;40:343–6.
14. Nakamura S, Matsumoto T, Umeno J, Yanai S, Shono Y, Suekane H, et al. Endoscopic features of intestinal follicular lymphoma: the value of double-balloon enteroscopy. Endoscopy. 2007;39(Suppl 1):E26–7.
15. Shia J, Teruya-Feldstein J, Pan D, Hegde A, Klimstra DS, Chaganti RS, et al. Primary follicular lymphoma of the gastrointestinal tract: a clinical and pathologic study of 26 cases. Am J Surg Pathol. 2002;26:216–24.
16. Huang WT, Hsu YH, Yang SF, Chuang SS. Primary gastrointestinal follicular lymphoma: a clinicopathologic study of 13 cases from Taiwan. J Clin Gastroenterol. 2008;42:997–1002.
17. Sentani K, Maeshima AM, Nomoto J, Maruyama D, Kim SW, Watanabe T, et al. Follicular lymphoma of the duodenum: a clinicopathologic analysis of 26 cases. Jpn J Clin Oncol. 2008;38:547–52.
18. Sato Y, Ichimura K, Tanaka T, Takata K, Morito T, Sato H, et al. Duodenal follicular lymphomas share common characteristics with mucosa-associated lymphoid tissue lymphomas. J Clin Pathol. 2008;6:377–81.
19. Toyoda H, Yamaguchi M, Nakamura S, Nakamura T, Kimura M, Suzuki H, et al. Regression of primary lymphoma of the ampulla of Vater after eradication of *Helicobacter pylori*. Gastrointest Endosc. 2001;54:92–6.
20. Kodama T, Ohshima K, Nomura K, Taniwaki M, Nakamura N, Nakamura S, et al. Lymphomatous polyposis of the gastrointestinal tract, including mantle cell lymphoma, follicular lymphoma and mucosa-associated lymphoid tissue lymphoma. Histopathology. 2005;47:467–78.
21. Kanda M, Ohshima K, Suzumiya J, Haraoka S, Kawasaki C, Sakisaka S, et al. Follicular lymphoma of the stomach: immunohistochemical and molecular genetic studies. J Gastroenterol. 2003;38:584–7.
22. Hashimoto Y, Nakamura N, Kuze T, Ono N, Abe M. Multiple lymphomatous polyposis of the gastrointestinal tract is a heterogenous group that includes mantle cell lymphoma and follicular lymphoma: Analysis of somatic mutation of immunoglobulin heavy chain gene variable region. Hum Pathol. 1999;30:581–7.
23. Nakase H, Matsuura M, Mikami S, Chiba T. Magnified endoscopic view of primary follicular lymphoma at the duodenal papilla. Intern Med. 2007;46:141–2.

24. Tanaka F, Tominaga K, Ochi M, Yamada T, Sasaki E, Shiba M, et al. Primary duodenal lymphoma: successful rituximab treatment and evaluation by FDG-PET. Hepatogastroenterology. 2007;54:1658–61.
25. Higuchi K, Komatsu K, Wakamatsu H, Kawasaki H, Murata M, Miyazaki K, et al. Small intestinal follicular lymphoma with multiple tumor formations diagnosed by double-balloon enteroscopy. Intern Med. 2007;46:705–9.
26. Tanaka S, Onoue G, Fujimoto T, Kosaka T, Yamasaki H, Yasui Y, et al. A case of primary follicular lymphoma in the duodenum confined to the mucosal layer. J Clin Gastroenterol. 2002;35:285–6.
27. Yamamoto S, Nakase H, Kawanami C. Follicular lymphoma with small intestinal involvement detected by double-balloon enteroscopy. Clin Gastroenterol Hepatol. 2007;5:A24.
28. Zenda T, Masunaga T, Fuwa B, Okada T, Ontachi Y, Kondo Y, et al. Small follicular lymphoma arising near the ampulla of Vater: a distinct subtype of duodenal lymphoma? Int J Gastrointest Cancer. 2005;36:113–9.
29. Matsuura M, Nakase H, Mochizuki N. Ileal polyposis caused by follicular lymphoma. Clin Gastroenterol Hepatol. 2007;5:e30.
30. Sakata Y, Iwakiri R, Sakata H, Fujisaki J, Mizuguchi M, Fukushima N, et al. Primary gastrointestinal follicular center lymphoma resembling multiple lymphomatous polyposis. Dig Dis Sci. 2001;46:567–70.
31. Takamura M, Narisawa R, Maruyama Y, Yokoyama J, Fukuhara Y, Kawai H, et al. A primary follicular lymphoma of the duodenum treated successfully with radiation therapy. Intern Med. 2006;45:309–11.
32. Higuchi N, Sumida Y, Nakamura K, Itaba S, Yoshinaga S, Mizutani T, et al. Impact of double-balloon endoscopy on the diagnosis of jejunoileal involvement in primary intestinal follicular lymphomas: a case series. Endoscopy. 2009;41:175–8.
33. Matsuzawa M, Shimodaira K, Nakamura N, Ochi Y, Hosaka S, Kiyosawa K, et al. A case of primary follicular lymphoma of the duodenum with BCL-2 gene rearrangement. J Gastroenterol. 2003;38:512–3.
34. Nomura K, Sekoguchi S, Ueda K, Nakao M, Akano Y, Fujita Y, et al. Differentiation of follicular from mucosa-associated lymphoid tissue lymphoma by detection of *t*(14;18) on single-cell preparations and paraffin-embedded sections. Genes Chromosomes Cancer. 2002;33:213–6.
35. Yoshida N, Nomura K, Matsumoto Y, Nishida K, Wakabayashi N, Konishi H, et al. Detection of BCL2-IGH rearrangement on paraffin-embedded tissue sections obtained from a small submucosal tumor of the rectum in a patient with recurrent follicular lymphoma. World J Gastroenterol. 2004;10:2602–4.
36. Tanaka S, Nagahara T, Hirakawa T, Ohta T, Fujimoto T, Takada R. Follicular lymphoma of the rectum. Intern Med. 2008;47:1277–8.
37. Takada M, Yamamoto S. Gastric follicular lymphoma with mediastinal lymph node dissemination detected by FDG-PET. Endoscopy. 2010; in press.
38. Inoue N, Isomoto H, Shikuwa S, Mizuta Y, Hayashi T, Kohno S. Magnifying endoscopic observation of primary follicular lymphoma of the duodenum by using the narrow-band imaging system. Gastrointest Endosc. 2009;69:158–9.
39. Esaki M, Matsumoto T, Nakamura S, Suekane H, Ohji Y, Yao T, et al. Capsule endoscopy findings in intestinal follicular lymphoma. Endoscopy. 2007;39(Suppl 1):E86–7.
40. van Deursen CT, Goedhard JG, Jie KS, Theunissen P. Primary intestinal follicular lymphoma diagnosed by video capsule endoscopy and double-balloon enteroscopy. Endoscopy. 2008;40(Suppl 2):E8–9.
41. Sapoznikov B, Morgenstern S, Raanani P, Aviram A, Rabizadeh E, Prokocimer M, et al. Follicular lymphoma with extensive gastrointestinal tract involvement: follow-up by capsule endoscopy. Dig Dis Sci. 2007;52:1031–5.
42. Ahmed S, Singh A, Krauss J, Wentz T, Gunaratnam NT. Successful treatment of refractory low grade duodenal lymphoma with rituximab, an anti-CD20 monoclonal antibody. Am J Clin Oncol. 2003;26:408–10.
43. Peters JH, Rondonotti E, Weijmer MC, Mulder CJ, Jacobs MA. Lymphomatous polyposis of the small intestine. Gastrointest Endosc. 2008;67:763–5.
44. Hoffmann M, Chott A, Püspök A, Jäger U, Kletter K, Raderer M. 18F-fluorodeoxyglucose positron emission tomography (18F-FDG-PET) does not visualize follicular lymphoma of the duodenum. Ann Hematol. 2004;83:276–8.
45. Bende RJ, Smit LA, Bossenbroek JG, Aarts WM, Spaargaren M, de Leval L, et al. Primary follicular lymphoma of the small intestine alpha4beta7 expression and immunoglobulin configuration suggest an origin from local antigen-experienced B cells. Am J Pathol. 2003;162:105–13.
46. Chuang SS, Chang ST, Liu H, Ye H, Sheu MJ, Chen MJ, et al. Intramucosal follicular lymphoma in the terminal ileum with nodal involvement. Pathol Res Pract. 2007;203:691–4.
47. Moynihan MJ, Bast MA, Chan WC, Jan Delabie, Wickert RS, Wu G, et al. Lymphomatous polyposis. A neoplasm of either follicular mantle or germinal center cell origin. Am J Surg Pathol. 1996;20:442–52.
48. Tzankov A, Hittmair A, Müller-Hermelink HK, Rüdiger T, Dirnhofer S. Primary gastric follicular lymphoma with parafollicular monocytoid B-cells and lymphoepithelial lesions, mimicking extranodal marginal zone lymphoma of MALT. Virchows Arch. 2002;441:614–7.
49. Straka C, Mielke B, Eichelmann A, Trede I, Ho AD, Möller P. Bcl-2 gene rearrangements in primary B-cell lymphoma of the gastrointestinal tract reveal follicular lymphoma as a subtype. Leukemia. 1993;7:268–73.
50. Tang Z, Jing W, Lindeman N, Harris NL, Ferry JA. One patient, two lymphomas. Simultaneous primary gastric marginal zone lymphoma and primary duodenal follicular lymphoma. Arch Pathol Lab Med. 2004;128:1035–8.
51. Freeman HJ, Anderson ME, Gascoyne RD. Clinical, pathological and molecular genetic findings in small intestinal follicle centre cell lymphoma. Can J Gastroenterol. 1997;11:31–4.
52. Rosty C, Brière J, Cellier C, Delabesse E, Carnot F, Barbier JP, et al. Association of a duodenal follicular lymphoma and hereditary nonpolyposis colorectal cancer. Mod Pathol. 2000;13:586–90.
53. Nadal E, Martinez A, Jiménez M, Ginés A, Campo E, Piqué J, et al. Primary follicular lymphoma arising in the ampulla of Vater. Ann Hematol. 2002;81:228–31.
54. Poggi MM, Cong PJ, Coleman CN, Jaffe ES. Low-grade follicular lymphoma of the small intestine. J Clin Gastroenterol. 2002;34:155–9.
55. Born P, Vieth M, Stolte M. Follicular lymphoma of the duodenum. Endoscopy. 2007;39(Suppl 1):E39.
56. Aguiar-Bujanda D, Quiñones-Morales I, Camacho-Galán R, Llorca-Martínez I, Rivero-Vera JC, Bohn-Sarmiento U, et al. Primary duodenal follicular lymphoma successfully treated with rituximab. Clin Transl Oncol. 2007;9:471–2.
57. Misdraji J, Fernandez del Castillo C, Ferry JA. Follicle center lymphoma of the ampulla of Vater presenting with jaundice: report of a case. Am J Surg Pathol. 1997;21:484–8.
58. Gallagher CJ, Gregory WM, Jones AE, Stansfeld AG, Richards MA, Dhaliwal HS, et al. Follicular lymphoma: prognostic factors for response and survival. J Clin Oncol. 1986;4:1470–80.

59. Armitage JO, Weisenburger DD. New approach to classifying non-Hodgkin's lymphomas: clinical features of the major histologic subtypes. Non-Hodgkin's Lymphoma Classification Project. J Clin Oncol. 1998;16:2780–95.
60. Carbone PP, Kaplan HS, Musshoff K, Smithers DW, Tubiana M. Report of the committee on Hodgkin's disease staging classification. Cancer Res. 1971;31:1860–1.
61. Rohatiner A, d'Amore F, Coiffier B, Crowther D, Gospodarowicz M, Isaacson P, et al. Report on a workshop convened to discuss the pathological and staging classifications of gastrointestinal tract lymphoma. Ann Oncol. 1994;5: 397–400.
62. The Non-Hodgkin's Lymphoma Classification Project. A clinical evaluation of the International Lymphoma Study Group classification of non-Hodgkin's lymphoma. The Non-Hodgkin's Lymphoma Classification Project. Blood. 1997;89:3909–18.
63. Takata K, Sato Y, Nakamura N, Kikuti YY, Ichimura K, Tanaka T, et al. Duodenal and nodal follicular lymphomas are distinct: the former lacks activation-induced cytidine deaminase and follicular dendritic cells despite ongoing somatic hypermutations. Mod Pathol. 2009;22:940–9.
64. Cruveilhier J. Maladies de l'estomac et des intestines. In: Cruveilhier J, editor. Anatomic pathologique du corps humain, vol 2, Sect. 34. Paris: JB Balliere; 1835–1842. p. 1–6.
65. Cornes JS. Multiple lymphomatous polyposis of the gastrointestinal tract. Cancer. 1961;14:249–57.
66. Isaacson PG, MacLennan KM, Subbuswamy SG. Multiple lymphomatous polyposis of the gastrointestinal tract. Histopathology. 1984;8:641–56.
67. Yatabe Y, Nakamura S, Nakamura T, Seto M, Ogura M, Kimura M, et al. Multiple polypoid lesions of primary mucosa-associated lymphoid-tissue lymphoma of colon. Histopathology. 1998;32:116–25.
68. Dawson IM, Cornes JS, Morson BC. Primary malignant lymphoid tumours of the intestinal tract. Report of 37 cases with a study of factors influencing prognosis. Br J Surg. 1961;49:80–9.
69. Iddan G, Meron G, Glukhovsky A, Swain P. Wireless capsule endoscopy. Nature. 2000;405:417.
70. Swain P. Wireless capsule endoscopy. Gut. 2003;52(Suppl 4):48–50.
71. Yamamoto H, Yano T, Kita H, Sunada K, Ido K, Sugano K. New system of double-balloon enteroscopy for diagnosis and treatment of small intestine disorders. Gastroenterology. 2003;125:1556–7.
72. Cerroni L, Arzberger E, Pütz B, Höfler G, Metze D, Sander CA, et al. Primary cutaneous follicle center cell lymphoma with follicular growth pattern. Blood. 2000;95:3922–8.
73. Franco R, Fernandez-Vazquez A, Rodriguez-Peralto JL, Bellas C, Lopez-Rios F, Saez A, et al. Cutaneous follicular B-cell lymphoma: description of a series of 18 cases. Am J Surg Pathol. 2001;25:875–83.
74. Bergman R, Kurtin PJ, Gibson LE, Hull PR, Kimlinger TK, Schroeter AL. Clinicopathologic, immunophenotypic, and molecular characterization of primary cutaneous follicular B-cell lymphoma. Arch Dermatol. 2001;137:432–9.
75. Child FJ, Russell-Jones R, Woolford AJ, Calonje E, Photiou A, Orchard G, et al. Absence of the $t(14;18)$ chromosomal translocation in primary cutaneous B-cell lymphoma. Br J Dermatol. 2001;144:735–44.
76. Harris NL, Ferry JA. Follicular lymphoma. In: Knowles DM, editor. Neoplastic hematopathology. 2nd ed. Baltimore: Lippincott Williams and Wilkins; 2001. p. 823–53.
77. Takeshita M, Iwashita A, Kurihara K, Ikejiri K, Higashi H, Udoh T, et al. Histologic and immunohistologic findings and prognosis of 40 cases of gastric large B-cell lymphoma. Am J Surg Pathol. 2000;24:1641–9.
78. Mann R, Berard C. Criteria for the cytologic subclassification of follicular lymphomas: a proposed alternative method. Hematol Oncol. 1982;1:187–92.
79. Nathwani BN, Metter GE, Miller TP, Burke JS, Mann RB, Barcos M, et al. What should be the morphologic criteria for the subdivision of follicular lymphomas? Blood. 1986;68: 837–45.
80. Anderson JR, Vose JM, Bierman PJ, Weisenberger DD, Sanger WG, Pierson J, et al. Clinical features and prognosis of follicular large-cell lymphoma: a report from the Nebraska Lymphoma Study Group. J Clin Oncol. 1993;11:218–24.
81. Ott G, Katzenberger T, Lohr A, Kindelberger S, Rüdiger T, Wilhelm M, et al. Cytomorphologic, immunohistochemical, and cytogenetic profiles of follicular lymphoma: 2 types of follicular lymphoma grade 3. Blood. 2002;99:3806–12.
82. de Leon ED, Alkan S, Huang JC, Hsi ED. Usefulness of an immunohistochemical panel in paraffin-embedded tissues for the differentiation of B-cell non-Hodgkin's lymphomas of small lymphocytes. Mod Pathol. 1998;11:1046–51.
83. Yunis JJ, Frizzera G, Oken MM, McKenna J, Theologides A, Arnesen M. Multiple recurrent genomic defects in follicular lymphoma. A possible model for cancer. N Engl J Med. 1987;316:79–84.
84. Bakhshi A, Jensen JP, Goldman P, Wright JJ, McBride OW, Epstein AL, et al. Cloning the chromosomal breakpoint of $t(14;18)$ human lymphomas: clustering around JH on chromosome 14 and near a transcriptional unit on 18. Cell. 1985; 41:899–906.
85. Cleary ML, Smith SD, Sklar J. Cloning and structural analysis of cDNAs for bcl-2 and a hybrid bcl-2/immunoglobulin transcript resulting from the $t(14;18)$ translocation. Cell. 1986;47: 19–28.
86. Weinberg OK, Ai WZ, Mariappan MR, Shum C, Levy R, Arber DA. "Minor" BCL2 breakpoints in follicular lymphoma: frequency and correlation with grade and disease presentation in 236 cases. J Mol Diagn. 2007;9:530–7.
87. Barrans SL, Evans PA, O'Connor SJ, Owen RG, Morgan GJ, Jack AS. The detection of $t(14;18)$ in archival lymph nodes: development of a fluorescence in situ hybridization (FISH)-based method and evaluation by comparison with polymerase chain reaction. J Mol Diagn. 2003;5:168–75.
88. Belaud-Rotureau MA, Parrens M, Carrere N, Turmo M, Ferrer J, de Mascarel A, et al. Interphase fluorescence in situ hybridization is more sensitive than BIOMED-2 polymerase chain reaction protocol in detecting IGH-BCL2 rearrangement in both fixed and frozen lymph node with follicular lymphoma. Hum Pathol. 2007;38:365–72.
89. Einerson RR, Kurtin PJ, Dayharsh GA, Kimlinger TK, Remstein ED. FISH is superior to PCR in detecting $t(14;18)(q32;q21)$-IgH/bcl-2 in follicular lymphoma using paraffin-embedded tissue samples. Am J Clin Pathol. 2005;124:421–9.
90. Tsujimoto Y, Cossman J, Jaffe E, Croce CM. Involvement of the bcl-2 gene in human follicular lymphoma. Science. 1985;228: 1440–3.
91. Buchonnet G, Jardin F, Jean N, Bertrand P, Parmentier F, Tison S, et al. Distribution of BCL2 breakpoints in follicular lymphoma and correlation with clinical features: specific subtypes or same disease? Leukemia. 2002;16:1852–6.
92. Cleary ML, Galili N, Sklar J. Detection of a second $t(14;18)$ breakpoint cluster region in human follicular lymphomas. J Exp Med. 1986;164:315–20.
93. Buchonnet G, Lenain P, Ruminy P, Lepretre S, Stamatoullas A, Parmentier F, et al. Characterization of BCL2-JH rearrangements in follicular lymphoma: PCR detection of 3' BCL2 breakpoints and evidence of a new cluster. Leukemia. 2000;14:1563–9.

94. Willis TG, Jadayel DM, Coignet LJ, Abdul-Rauf M, Treleaven JG, Catovsky D, et al. Rapid molecular cloning of rearrangements of the IGHJ locus using long-distance inverse polymerase chain reaction. Blood. 1997;90:2456–64.
95. Akasaka T, Akasaka H, Yonetani N, Ohno H, Yamabe H, Fukuhara S, et al. Refinement of the BCL2/immunoglobulin heavy chain fusion gene in *t*(14;18)(q32;q21) by polymerase chain reaction amplification for long targets. Genes Chromosomes Cancer. 1998;21:17–29.
96. Gu K, Chan WC, Hawley RC. Practical detection of *t*(14;18) (IgH/BCL2) in follicular lymphoma. Arch Pathol Lab Med. 2008;132:1355–61.
97. Kumar R, Maillard I, Schuster SJ, Alavi A. Utility of fluorodeoxyglucose-PET imaging in the management of patients with Hodgkin's and non-Hodgkin's lymphomas. Radiol Clin North Am. 2004;42:1083–100.
98. Burton C, Ell P, Linch D. The role of PET imaging in lymphoma. Br J Haematol. 2004;126:772–84.
99. Naumann R, Vaic A, Beuthien-Baumann B, Bredow J, Kropp J, Kittner T, et al. Prognostic value of positron emission tomography in the evaluation of post-treatment residual mass in patients with Hodgkin's disease and non-Hodgkin's lymphoma. Br J Haematol. 2001;115:793–800.
100. Tsukamoto N, Kojima M, Hasegawa M, Oriuchi N, Matsushima T, Yokohama A, et al. The usefulness of 18F-fluorodeoxyglucose positron emission tomography (18F-FDG-PET) and a comparison of 18F-FDG-PET with 67gallium scintigraphy in the evaluation of lymphoma: relation to histologic subtypes based on the World Health Organization Classification. Cancer. 2007;110:652–9.
101. Karam M, Novak L, Cyriac J, Ali A, Nazeer T, Nugent F. Role of fluorine-18 fluoro-deoxyglucose positron emission tomography scan in the evaluation and follow-up of patients with low-grade lymphomas. Cancer. 2006;107:175–83.
102. Wöhrer S, Jaeger U, Kletter K, Becherer A, Hauswirth A, Turetschek K, et al. 18F-fluoro-deoxy-glucose positron emission tomography (18F-FDG-PET) visualizes follicular lymphoma irrespective of grading. Ann Oncol. 2006;17:780–4.
103. Federico M, Vitolo U, Zinzani PL, Chisesi T, Clò V, Bellesi G, et al. Prognosis of follicular lymphoma: a predictive model based on a retrospective analysis of 987 cases. Intergruppo Italiano Linfomi. Blood. 2000;95:783–9.
104. Solal-Céligny P, Roy P, Colombat P, White J, Armitage JO, Arranz-Saez R, et al. Follicular lymphoma international prognostic index. Blood. 2004;104:1258–65.
105. Decaudin D, Lepage E, Brousse N, Brice P, Harousseau JL, Belhadj K, et al. Low-grade stage III-IV follicular lymphoma: multivariate analysis of prognostic factors in 484 patients—a study of the groupe d'Etude des lymphomes de l'Adulte. J Clin Oncol. 1999;17:2499–505.
106. Ardeshna KM, Smith P, Norton A, Hancock BW, Hoskin PJ, MacLennan KA, et al. Long-term effect of a watch and wait policy versus immediate systemic treatment for asymptomatic advanced-stage non-Hodgkin lymphoma: a randomized controlled trial. Lancet. 2003;362:516–22.
107. Brandt L, Kimby E, Nygren P, Glimelius B. A systematic overview of chemotherapy effects in indolent non-Hodgkin's lymphoma. Acta Oncol. 2001;40:213–23.
108. Johnson PW, Rohatiner AZ, Whelan JS, Price CG, Love S, Lim J, et al. Patterns of survival in patients with recurrent follicular lymphoma: a 20-year study from a single center. J Clin Oncol. 1995;13:140–7.
109. Marcus R, Imrie K, Belch A, Cunningham D, Flores E, Catalano J, et al. CVP chemotherapy plus rituximab compared with CVP as first-line treatment for advanced follicular lymphoma. Blood. 2005;105:1417–23.
110. Hiddemann W, Kneba M, Dreyling M, Schmitz N, Lengfelder E, Schmits R, et al. Frontline therapy with rituximab added to the combination of cyclophosphamide, doxorubicin, vincristine, and prednisone (CHOP) significantly improves the outcome for patients with advanced-stage follicular lymphoma compared with therapy with CHOP alone: results of a prospective randomized study of the German Low-Grade Lymphoma Study Group. Blood. 2005;106:3725–32.
111. Herold M, Haas A, Srock S, Neser S, Al-Ali KH, Neubauer A, et al. Rituximab added to first-line mitoxantrone, chlorambucil, and prednisolone chemotherapy followed by interferon maintenance prolongs survival in patients with advanced follicular lymphoma: an East German Study Group Hematology and Oncology Study. J Clin Oncol. 2007;25:1986–92.
112. Wotherspoon AC, Ortiz-Hidalgo C, Falzon MR, Isaacson PG. *Helicobacter pylori*-associated gastritis and primary B-cell gastric lymphoma. Lancet. 1991;338:1175–6.
113. Farinha P, Gascoyne RD. *Helicobacter pylori* and MALT lymphoma. Gastroenterology. 2005;128:1579–605.
114. Parsonnet J, Hansen S, Rodriguez L, Gelb AB, Warnke RA, Jellum E, et al. *Helicobacter pylori* infection and gastric lymphoma. N Engl J Med. 1994;330:1267–71.
115. Hussell T, Isaacson PG, Crabtree JE, Spencer J. The response of cells from low-grade B-cell gastric lymphomas of mucosa-associated lymphoid tissue to *Helicobacter pylori*. Lancet. 1993;342:571–4.
116. Wotherspoon AC, Doglioni C, Diss TC, Pan L, Moschini A, de Boni M, et al. Regression of primary low-grade B-cell gastric lymphoma of mucosa-associated lymphoid tissue type after eradication of *Helicobacter pylori*. Lancet. 1993;342:575–7.
117. Bayerdorffer E, Neubauer A, Rudolph B, Thiede C, Lehn N, Eidt S, et al. Regression of primary gastric lymphoma of mucosa-associated lymphoid tissue type after cure of *Helicobacter pylori* infection. MALT Lymphoma Study Group. Lancet. 1995;345:1591–4.
118. Roggero E, Zucca E, Pinotti G, Pascarella A, Capella C, Savio A, et al. Eradication of *Helicobacter pylori* infection in primary low-grade gastric lymphoma of mucosa-associated lymphoid tissue. Ann Intern Med. 1995;122:767–9.
119. Neubauer A, Thiede C, Morgner A, Alpen B, Ritter M, Neubauer B, et al. Cure of *Helicobacter pylori* infection and duration of remission of low-grade gastric mucosa-associated lymphoid tissue lymphoma. J Natl Cancer Inst. 1997;89:1350–5.
120. Savio A, Zamboni G, Capelli P, Negrini R, Santandrea G, Scarpa A, et al. Relapse of low grade gastric MALT lymphoma after *Helicobacter pylori* eradication: true relapse or persistence? Long-term posttreatment follow-up of a multicenter trial in the north-east of Italy and evaluation of the diagnostic protocol's adequacy. Recent Results Cancer Res. 2000;156:116–24.
121. Fischbach W, Goebeler-Kolve ME, Dragosics B, Greiner A, Stolte M. Long term outcome of patients with gastric marginal zone B cell lymphoma of mucosa associated lymphoid tissue (MALT) following exclusive *Helicobacter pylori* eradication therapy: experience from a large prospective series. Gut. 2004;53:34–7.
122. Wundisch T, Thiede C, Morgner A, Dempfle A, Gunther A, Liu H, et al. Long-term follow-up of gastric MALT lymphoma after *Helicobacter pylori* eradication. J Clin Oncol. 2005;23:8018–24.
123. Seligmann M, Danon F, Hurez D, Mihaesco E, Preud'homme JL. Alpha-chain disease: a new immunoglobulin abnormality. Science. 1968;162:1396–7.
124. Rambaud J, Halphen M. Immunoproliferative small intestinal disease (IPSID): relationships with alpha-chain disease and "Mediterranean" lymphomas. Gastroenterol Int. 1989;2:33–41.

125. Lecuit M, Abachin E, Martin A, Poyart C, Pochart P, Suarez F, et al. Immunoproliferative small intestinal disease associated with *Campylobacter jejuni*. N Engl J Med. 2004;350:239–48.

126. Suarez F, Lortholary O, Hermine O, Lecuit M. Infection-associated lymphomas derived from marginal zone B cells: a model of antigen-driven lymphoproliferation. Blood. 2006;107:3034–44.

9 Schöniger-Hekele M, Petermann D, Weber B, Müller C. Tropheryma whipplei in the environment: survey of sewage plant influxes and sewage plant workers. Appl Environ Microbiol 2007;73:2033–5.

10 Schneider T, Moos V, Loddenkemper C, Marth T, Fenollar F, Raoult D. Whipple's disease: new aspects of pathogenesis and treatment. Lancet Infect Dis 2008;8: 179–90.

Rheumatology 2010;49:1602–1604
doi:10.1093/rheumatology/keq080
Advance Access publication 12 April 2010

Enhanced cytokine responses to Toll-like and NOD-like receptor ligands in primary biliary cirrhosis–CREST overlap syndrome

SIR, Although clinical features of the CREST syndrome are sometimes exhibited in patients with primary biliary cirrhosis (PBC), the mechanisms behind these overlap conditions are poorly understood. Recent studies suggest the involvement of hyper-responsiveness to Toll-like receptor (TLR) signalling in PBC and scleroderma [1, 2]. Here, we report a patient with PBC-CREST overlap syndrome showing enhanced innate immune responses to TLR and NOD-like receptor (NLR) ligands.

A 72-year-old Japanese woman was admitted for further examination of liver dysfunction. She had been suffering from RP and sclerodactyly for 10 years. Barium swallow performed for the investigation of nausea showed a dilated oesophagus and diminished peristalsis due to oesophageal dysmotility. Biochemical values showed elevated levels of serum hepatobiliary enzymes (aspartate transaminase 171 IU/l, alanine aminotransferase 171 IU/l, alkaline phosphatase 1595 IU/l, γ-glutamyl transpeptidase 612 IU/l). Serological tests for hepatitis B and C virus were negative. A marked elevation of serum ANA and ACA titre was seen (×1280). AMA was also positive. Antibodies against ssDNA and dsDNA, Scl-70, Jo-1, RNP, Sm, liver/kidney microsome type-1, and SSA and SSB antigens were negative. Histopathology of the liver biopsy specimen showed destruction of intrahepatic bile ducts by infiltration of mononuclear inflammatory cells and findings are consistent with chronic non-suppurative destructive cholangitis in PBC (Fig. 1A). She was diagnosed as PBC-CREST overlap syndrome based on these results.

Monocytes from patients with PBC exhibit enhanced pro-inflammatory cytokine responses to TLR ligands, suggesting that over-reactivity to microbial antigens underlies the immunopathogenesis of PBC [1]. In addition, activation of Type I IFN signalling mediated by nucleic acid-containing immune complex is associated with development of scleroderma [2]. However, it is unknown which type of immune response is predominant in patients with PBC-CREST overlap syndrome. $CD14^+$ monocytes were isolated from peripheral blood mononuclear cells of this patient and two healthy controls to measure the production of pro-inflammatory cytokines upon stimulation with microbial antigens after written informed consent was obtained according to the Declaration of Helsinki. The design of the work conforms to standards currently applied in Kyoto University. Monocytes (1×10^6/ml) were stimulated with a broad range of TLR and NLR ligands [FK156, NOD1 ligand, 10 μg/ml; muramyl dipeptide (MDP), NOD2 ligand, 10 μg/ml; Pam_3CSK4 (PAM), TLR2 ligand, 1 μg/ml; lipopolysaccharide (LPS), TLR4 ligand, 1 μg/ml; and flagellin, TLR5 ligand, 1 μg/ml] for 24 h [3–5]. Monocytes from the patient showed enhanced production of IL-6 upon stimulation with TLR2, TLR4 and TLR5 ligands as compared with those from healthy controls (Fig. 1B). Not only TLR but also NLR (NOD1 and NOD2) ligands enhanced IL-8 production by monocytes from the patient. Interestingly, production of IFN-β was markedly enhanced by stimulation with TLR3 and TLR4 ligands in monocytes from the patient. Thus, monocytes from the patient with PBC-CREST overlap syndrome were characterized by enhanced pro-inflammatory cytokine and Type I IFN responses to microbial antigens.

Production of IL-6 and IFN-β depends upon activation of nuclear factor-kappa B (NF-κB) and IRF3, respectively [6]. We next addressed whether enhanced cytokine responses in this patient was associated with transactivation of these transcription factors. For this purpose, nuclear extracts (20 μg) isolated from monocytes after stimulation with TLR3 and TLR4 ligands for 1 h were subjected to transfactor binding assay [3–5]. Nuclear translocation of NF-κB subunit, p65 and IRF3 was markedly enhanced in monocytes from the patient upon stimulation with TLR3 and TLR4 ligands as compared with healthy controls (Fig. 1C). These data suggest that enhanced activation of NF-κB and IRF3 via TLR signalling causes a robust production of IL-6 and IFN-β by monocytes from the patient.

We have found that monocytes from the patient with PBC-CREST overlap syndrome show hyper-reactivity to both TLR and NLR ligands in terms of pro-inflammatory cytokine and IFN-β responses. Production of IL-6 mediated by TLRs is up-regulated in PBC, whereas activation of Type I IFN signalling may be involved in scleroderma [1, 2]. In addition, Takii *et al.* [7] showed involvement of Type I IFN signalling via TLR3 in the pathogenesis of PBC. Thus, activation of Type I IFN signalling is one of the characteristic findings in innate immune responses not only in scleroderma but also in PBC. The results of our study clearly show that monocytes from the patient with PBC-CREST overlap syndrome exhibit both phenotypes upon stimulation with TLR and NLR ligands since these microbial antigens induce increased production of both IL-6 and IFN-β. Patients with PBC-CREST overlap syndrome manifest features of both PBC and scleroderma not only in clinical symptoms but also in innate immune responses. In this regard, it is possible

Fig. 1 Enhanced cytokine responses to TLR and NLR ligands in a patient with PBC-CREST overlap syndrome. (**A**) Haematoxylin and eosin staining of liver biopsy specimen. Massive infiltration of inflammatory cells, which mainly consists of lymphocytes, was seen around the bile ducts. (**B**) $CD14^+$ monocytes were isolated from two healthy controls and the patient. These $CD14^+$ monocytes (1×10^6/ml) were stimulated with TLR and NLR ligands (FK156 10 μg/ml, MDP 10 μg/ml, PAM 1 μg/ml, dsRNA 50 μg/ml, LPS 1 μg/ml and flagellin 1 μg/ml) for 24 h and then culture supernatants were subjected to IL-6, IL-8 and IFN-β assay. (**C**) Nuclear extracts were isolated from $CD14^+$ monocytes stimulated with dsRNA or LPS for 1 h as described in (B). Nuclear extracts (20 μg) were subjected to NF-κB and IRF3 activation assay. Results are expressed as mean (S.D.) and mean alone, respectively, in the control and patient's samples (B, C).

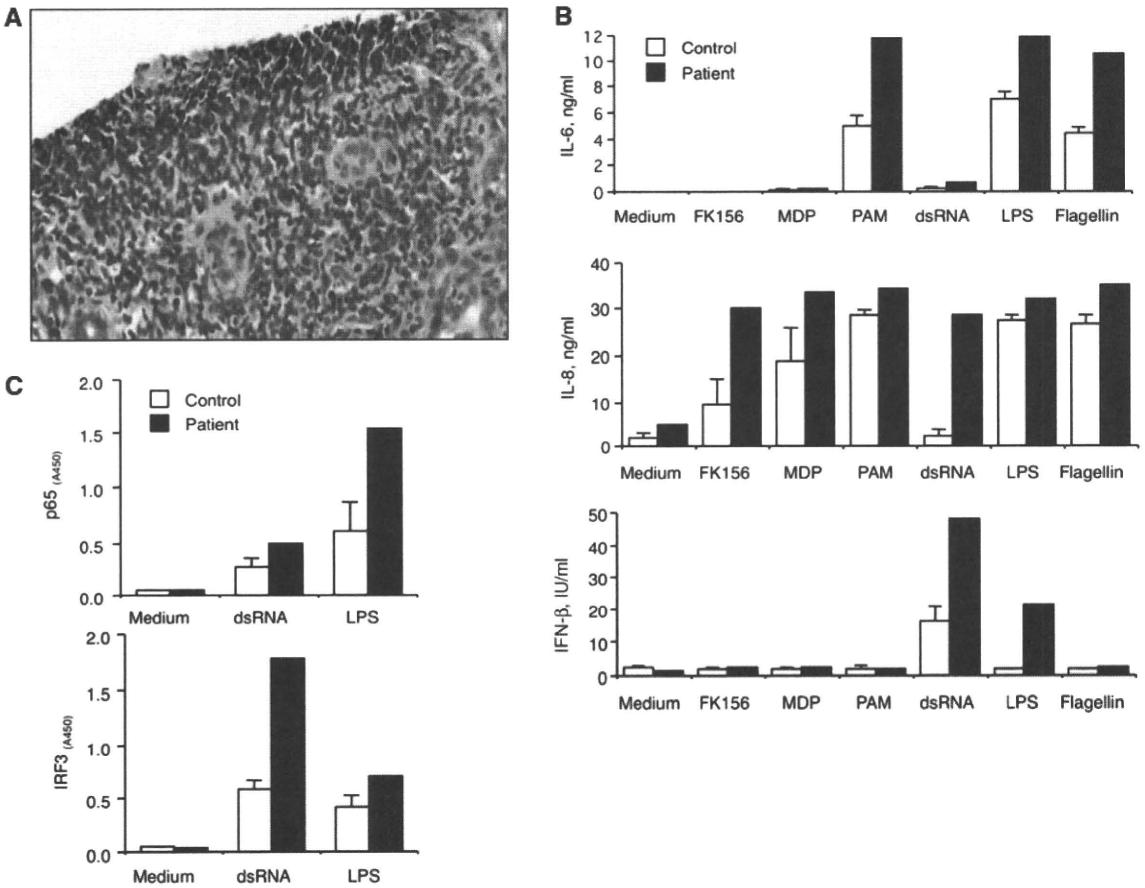

that activation of Type I IFN signalling, a common feature of innate immune responses in PBC and CREST syndrome, might have caused PBC-CREST overlap syndrome exhibiting enhanced activation of multiple TLR pathways. Another important issue arising from this study is whether microbial infections cause PBC-CREST overlap syndrome by the breakdown of self-tolerance through hyper-responsiveness to TLR and NLR ligands. In fact, molecular mimicry between microbial antigens and auto-antigens is considered as one possible mechanism of immunopathogenesis of PBC and scleroderma although a direct causal association between infections and these diseases is missing [8, 9].

In conclusion, we report the first case of a patient with PBC-CREST overlap syndrome exhibiting enhanced production of IL-6 and IFN-β to TLR and NLR ligands. It should be noted, however, that future studies using a large number of patients with PBC-CREST overlap syndrome are absolutely required to confirm this idea.

Rheumatology key message

- Innate immune responses mediated by TLRs and NLRs are enhanced in PBC-CREST overlap syndrome.

Disclosure statement: This work is supported in part by grants from Viral Hepatitis Research Foundation of Japan, Takeda Science Foundation and Uehara Memorial Foundation to T. W. All other authors have declared no conflicts of interest.

Manabu Fukuhara[1], Tomohiro Watanabe[1], Taro Ueo[1], Hiroshi Ida[1], Yuzo Kodama[1] and Tsutomu Chiba[1]

[1]*Department of Gastroenterology and Hepatology, Kyoto University Graduate School of Medicine, Kyoto, Japan.*
Accepted 18 February 2010
Correspondence to: Tomohiro Watanabe, Department of Gastroenterology and Hepatology, Kyoto University Graduate School of Medicine, 54 Shogoin Kawahara-cho, Sakyo-ku, Kyoto 606-8507, Japan.
E-mail: tmhrwtnb@kuhp.kyoto-u.ac.jp

References

1 Mao TK, Lian ZX, Selmi C *et al*. Altered monocyte responses to defined TLR ligands in patients with primary biliary cirrhosis. Hepatology 2005;42:802–8.
2 Lafyatis R, York M. Innate immunity and inflammation in systemic sclerosis. Curr Opin Rheumatol 2009;21: 617–22.
3 Watanabe T, Asano N, Murray PJ *et al*. Muramyl dipeptide activation of nucleotide-binding oligomerization domain 2 protects mice from experimental colitis. J Clin Invest 2008; 118:545–59.
4 Watanabe T, Kitani A, Murray PJ, Strober W. Nod2 is a negative regulator of Toll-like receptor 2-mediated T helper type 1 responses. Nat Immunol 2004;5:800–8.
5 Watanabe T, Kitani A, Murray PJ, Wakatsuki Y, Fuss IJ, Strober W. Nucleotide binding oligomerization domain 2 deficiency leads to dysregulated TLR2 signaling and induction of antigen-specific colitis. Immunity 2006;25: 473–85.
6 Akira S, Takeda K. Toll-like receptor signalling. Nat Rev Immunol 2004;4:499–511.
7 Takii Y, Nakamura M, Ito M *et al*. Enhanced expression of type I interferon and toll-like receptor-3 in primary biliary cirrhosis. Lab Invest 2005;85:908–20.
8 Shimoda S, Nakamura M, Ishibashi H *et al*. Molecular mimicry of mitochondrial and nuclear autoantigens in primary biliary cirrhosis. Gastroenterology 2003;124: 1915–25.
9 Randone SB, Guiducci S, Cerinic MM. Systemic sclerosis and infections. Autoimmun Rev 2008;8:36–40.

Rheumatology 2010;49:1604–1606
doi:10.1093/rheumatology/keq104
Advance Access publication 16 April 2010

Acute haemorrhagic oedema of infancy—a case of benign cutaneous leucocytoclastic vasculitis

SIR, This 10-month-old male infant presented with a 3-day history of erythematous, purpuric rash and progressive swelling of the limbs, 2 weeks after recovering from chicken pox. Blood tests revealed mildly deranged clotting: prothrombin time (PT) 12.2 s, activated partial thromboplastin time (APTT) 50.7 s and fibrinogen 6.5 g/l (normal range: PT 10.4–12.8, APTT 24–32.2 and fibrinogen 1.7–5.5). Due to concerns that the rash may represent purpura fulminans (PF), a rare but serious immune-mediated complication following chicken pox, he was referred to the regional tertiary paediatric unit.

On admission he was afebrile, alert but miserable, with well-defined tender erythematous palpable annular lesions with purpuric centres predominantly on the limbs (Fig. 1a), pale pink reticulate rash on left ear (Fig. 1b) and right ankle, and with marked oedema of limbs and was reluctant to move the left shoulder (Fig. 1c). He had scattered healing chicken pox lesions, shotty cervical and inguinal lymph nodes, but no respiratory or abdominal symptoms and no other joint pain. He was normotensive, urinalysis was negative and he had one episode of dark stool, but no fresh red blood.

A clinical diagnosis of acute haemorrhagic oedema of infancy (AHOI) was confirmed by skin biopsy demonstrating leucocytoclastic vasculitis, involving small blood vessels in the dermis and superficial subcutis, with perivascular neutrophilc infiltrate (Fig. 1d). Immunoperoxidase staining performed on de-paraffinized sections using proteinase K pre-digestion showed fine granular IgA deposits around some small blood vessels in the dermis, with no specific binding of IgG, IgM or C3. Repeated extended clotting tests showed only slightly reduced free protein S (63%, range 75–142). ESR was elevated at 56 mm/h. Autoantibody screen, ANCA, aCL (IgG and IgM), serum immunoglobulin and complement C3 and C4 levels were negative or within normal range.

He was managed conservatively with i.v. fluids, pain control (paracetamol) and antibiotics (ceftriaxone initially, changed to oral amoxicillin after 2 days). He made a rapid recovery, remained afebrile, was eating and drinking within 1 day of admission and by Day 2 no new lesions were seen. He was discharged home, and the rash and oedema resolved completely within 2 weeks.

The uncommon presentation of acute leucocytoclastic vasculitis in infants and young children between 3 months and 2 years of age was first described in 1913 [1] and named as acute haemorrhagic oedema by Finkelstein in the late 1930s [2]. Our patient had typical presentation with rapid development of tender and well-demarcated rosette-like (*en cockade* after Seidlmayer) purpuric lesions associated with marked painful oedema [2]. The clinical triad of fever, painful skin lesions and oedema is characteristic. The head and distal limbs are the most common sites of presentation. Systemic involvement is rare, but haematuria, mild proteinuria and bloody diarrhoea as well as arthritis and arthalgia have been reported. Routine blood tests are essentially normal, except for a mildly elevated ESR. A profound leucocytoclastic vasculitis is usually seen on histology (Fig. 1d); IgM, C1q and fibrinogen are frequently found, and perivascular IgA deposition has been reported in ~25% of the cases [3], as in this case. The benign course is typical with spontaneous and complete resolution often occurring within 1–3 weeks, without specific treatment [3, 4].

The pathogenesis and aetiology of AHOI is unknown, but an IC-mediated vasculitis is most likely [5], as in the

IMMUNOLOGY

Distinct Signal Codes Generate Dendritic Cell Functional Plasticity

Kazuhiko Arima, Norihiko Watanabe,* Shino Hanabuchi, Mikyoung Chang, Shao-Cong Sun, Yong-Jun Liu†

(Published 19 January 2010; Volume 3 Issue 105 ra4)

Our adaptive immune system induces distinct responses to different pathogens because of the functional plasticity of dendritic cells (DCs); however, how DCs program unique responses remains unclear. Here, we found that the cytokine thymic stromal lymphopoietin (TSLP) potently transduced a unique T helper type 2 (T_H2)–inducing compound signal in DCs. Whereas activation of nuclear factor κB (predominantly p50) drove DCs to produce OX40L to induce T_H2 differentiation, the activation of signal transducer and activator of transcription 6 (STAT6) triggered DCs to secrete chemokines necessary for the recruitment of T_H2 cells. In addition, TSLP signaling limited the activation of STAT4 and interferon regulatory factor 8 (IRF-8), which are essential factors for the production of the T_H1-polarizing cytokine interleukin-12 (IL-12). By contrast, Toll-like receptor ligands and CD40 ligand did not activate STAT6 in myeloid DCs, but instead increased the abundance of STAT4 and IRF-8 to induce T_H1 responses through the production of IL-12. Therefore, we propose that the functional plasticity of DCs relies on elaborate signal codes that are generated by different stimuli.

INTRODUCTION

Dendritic cells (DCs) are professional antigen-presenting cells (APCs), which are characterized by a strong ability to stimulate the proliferation of T cells and by a functional plasticity in the induction of distinct T helper cell responses to different types of invading pathogens (*1*). Certain microbial components, such as ligands for Toll-like receptors (TLRs), and CD40 ligand (CD40L), which is on activated T cells, induce the maturation of DCs, a process by which immature DCs differentiate into fully competent APCs capable of priming T cell responses, and the production of the cytokine interleukin-12 (IL-12). IL-12 is indispensable for mounting T helper type 1 (T_H1) responses to eradicate most intracellular microbes by inducing the production of interferon-γ (IFN-γ) (*2*, *3*). By contrast, extracellular pathogens, such as helminths, and allergens induce distinct immune responses called T_H2 responses, which cause eosinophilic inflammation; however, the underlying molecular mechanisms that determine the functional plasticity of DCs are poorly understood (*4*–*8*).

Thymic stromal lymphopoietin (TSLP) is an IL-7–like cytokine that is a key molecule for initiating T_H2 responses (*9*). In humans, TSLP is produced predominantly by epithelial cells and activates myeloid DCs (mDCs) to induce T_H2 responses in T cells, which is associated with allergic inflammation (*9*). Inhibiting the function of TSLP in vivo has provided a promising therapeutic effect for allergic diseases (*10*, *11*). The ability of TSLP-activated mDCs (TSLP-mDCs) to induce T_H2 responses is directly linked to three unique features of these cells: (i) the secretion of chemokines that specifically attract T_H2 cells; (ii) the presence of the T_H2-polarizing molecule OX40 ligand (OX40L); and (iii) the inability to produce the T_H1-polarizing cytokine IL-12 (*12*–*14*). We wished to understand how TSLP receptor (TSLPR) signaling induced T_H2 responses so that we could try to uncover the molecular mechanisms responsible for the functional plasticity of DCs.

Department of Immunology and Center for Cancer Immunology Research, The University of Texas M. D. Anderson Cancer Center, 7455 Fannin, Unit 901, Houston, TX 77030, USA.
*Present address: Center for Innovation in Immunoregulative Technology and Therapeutics and Department of Gastroenterology and Hepatology, Graduate School of Medicine, Kyoto University, Kyoto 606-8501, Japan.
†To whom correspondence should be addressed. E-mail: yjliu@mdanderson.org

RESULTS

TSLP activates a distinct set of STAT proteins to program T_H2-inducing mDCs

Previous studies of cell lines that have the TSLPR complex, which consists of TSLPR and the α chains of the IL-7 receptor (IL-7Rα), showed that TSLP activates the transcription factors signal transducer and activator of transcription 3 (STAT3) and STAT5 (*15*, *16*). However, activation of these ubiquitous signaling molecules is unlikely to explain the unique features of TSLP-mDCs. STAT6 regulates the production of the T_H2 cell–attracting CC chemokine CCL17 [also known as thymus and activation-regulated chemokine (TARC)] in T cells and macrophages (*17*, *18*). We therefore examined the activation status of all of the STAT proteins in human mDCs after 24 hours of culture with TSLP, ligands for different TLRs, or CD40L (Fig. 1A). Phosphorylation of STAT1 and STAT3 was widely induced by TSLP and certain TLR ligands. In addition, TSLP induced the preferential phosphorylation of STAT5 and STAT6, which are involved in T_H2 responses (*19*), whereas the TLR3 agonist polyinosinic:polycytidylic acid [poly(I:C)] and the TLR7 and TLR8 agonist R848, two major stimuli of the production of IL-12p70 in human primary mDCs (*20*), induced the preferential phosphorylation of STAT2 and STAT4, key transcription factors that are involved in T_H1 responses (*5*). We occasionally observed that R848 also induced much weaker phosphorylation of STAT5 than did TSLP (fig. S1). CD40L did not induce detectable phosphorylation of any STAT protein.

To determine whether TSLP directly activated multiple STATs, mDCs were stimulated for up to 30 min with TSLP, poly(I:C), IFN-β, IL-4 (a cytokine that drives T_H2 responses), or bovine serum albumin (BSA) as a negative control (Fig. 1B). TSLP induced the phosphorylation of STAT1, -3, -4, -5, and -6 within 5 min, whereas poly(I:C) did not stimulate the phosphorylation of any STAT protein within 30 min, which suggests that poly(I:C) indirectly induces phosphorylation of STAT proteins at later time points,

possibly through an autocrine pathway that involves IFN-β (Fig. 1A) (*21*). Indeed, IFN-β induced the phosphorylation of STAT1, -2, -3, -4, and -5, whereas IL-4 stimulated the phosphorylation of STAT6 within 30 min, as was reported for other cell types (*22*). Phosphorylation of STAT6 is typically induced by IL-4Rα upon binding to IL-4 or IL-13 (*23*). TSLP-mediated phosphorylation of STAT6 was blocked by neutralizing antibodies against TSLPR but not by antibodies against IL-4Rα, whereas IL-4– and IL-13–mediated phosphorylation of STAT6 was blocked by antibodies against IL-4Rα but not by antibodies against TSLPR, indicating that TSLPR mediates the activation of STAT6 independently of IL-4Rα (Fig. 1C). Chromatin immunoprecipitation (ChIP) assays revealed the binding of TSLP-activated STAT6 to the promoter of *CCL17* (Fig. 1D), suggesting that the production of CCL17 by TSLP-mDCs (*9*) depends on TSLP-mediated activation of STAT6.

TSLP induces robust and sustained activation of Janus kinase 1 and 2 in mDCs

Cytokine-dependent activation of STATs is primarily mediated by Janus kinases (JAKs) (*22*–*24*); however, JAKs are not involved in TSLP signaling in mice (*15*). We therefore examined whether JAKs were activated by TSLP in human primary mDCs. Whereas IL-7 stimulated a weak and transient (<5 min) phosphorylation of JAK1, TSLP induced robust and sustained (~1 hour) phosphorylation of JAK1 and JAK2 in mDCs (Fig. 2A). This finding may explain why TSLP, but not other cytokines such as IL-7, could induce sustained (>2 hours) and broad activation of STATs (Figs. 1B and 2A and fig. S2). Because JAKs have the potential to activate several signaling pathways in addition to those involving STATs (*24*), we examined the activation of the phosphoinositide 3-kinase (PI3K)–Akt pathway and of mitogen-activated protein kinases (MAPKs) in response to TSLP and found that phosphorylation of Akt and the MAPKs extracellular signal–regulated kinase (ERK) and c-Jun N-terminal kinase (JNK) was rapidly induced by TSLP (Fig. 2B and fig. S3).

To confirm the role of JAKs in mediating the range of TSLP-dependent signals, mDCs were pretreated with the pan-JAK inhibitor pyridone 6, the PI3K inhibitor LY294002, the MEK (ERK) inhibitor U0126, or with dimethyl sulfoxide (DMSO) as the vehicle control and were then stimulated with TSLP or IL-1β, a cytokine that stimulates JAK-independent signaling. We found that the pan-JAK inhibitor completely blocked the TSLP-dependent phosphorylation of STATs, Akt, and ERK, whereas it did not block the IL-1β–dependent phosphorylation of ERK and only partially blocked the phosphorylation of Akt, indicating that the robust and broad signals in response to TSLP were dependent on the activation of JAKs (Fig. 2B). The PI3K inhibitor LY294002 did not block TSLP-dependent phosphorylation of STATs but blocked the phosphorylation of Akt and ERK in response to TSLP. In contrast, whereas LY294002 blocked the IL-1β–dependent phosphorylation of Akt, it did not block the phosphorylation of ERK in response to IL-1β, demonstrating that the TSLP-dependent activation of ERK required activation of the PI3K-Akt pathway. The MEK inhibitor blocked the phosphorylation of ERK in response to either TSLP or IL-1β, but it did not inhibit the TSLP-dependent phosphorylation of STAT and Akt, nor did it block the IL-1β–dependent phosphorylation of Akt. Collectively, these data suggest that JAKs constitute critical mediators of the broad signaling of TSLP in human mDCs.

TSLP induces the production of OX40L in mDCs by the sustained activation of p50 and RelB

Upon activation with TSLP, mDCs increase the abundance on their cell surface of molecules such as major histocompatibility complex II (MHC II), CD40, CD80, and CD86 in 24 hours and that of OX40L, a potent T_H2-polarizing molecule, in 48 to 72 hours (*9*, *12*, *13*). This increase in the abundance of the enrichment of STAT6 at the region around the STAT6 consensus elements (STAT6CE) of the promoter of *CCL17* in response to TSLP. A region ~6000 bp upstream of the initiator codon of the gene was used as negative control. Data are displayed as inverted images for easier visibility and are representative of three independent experiments. IgG, immunoglobulin G.

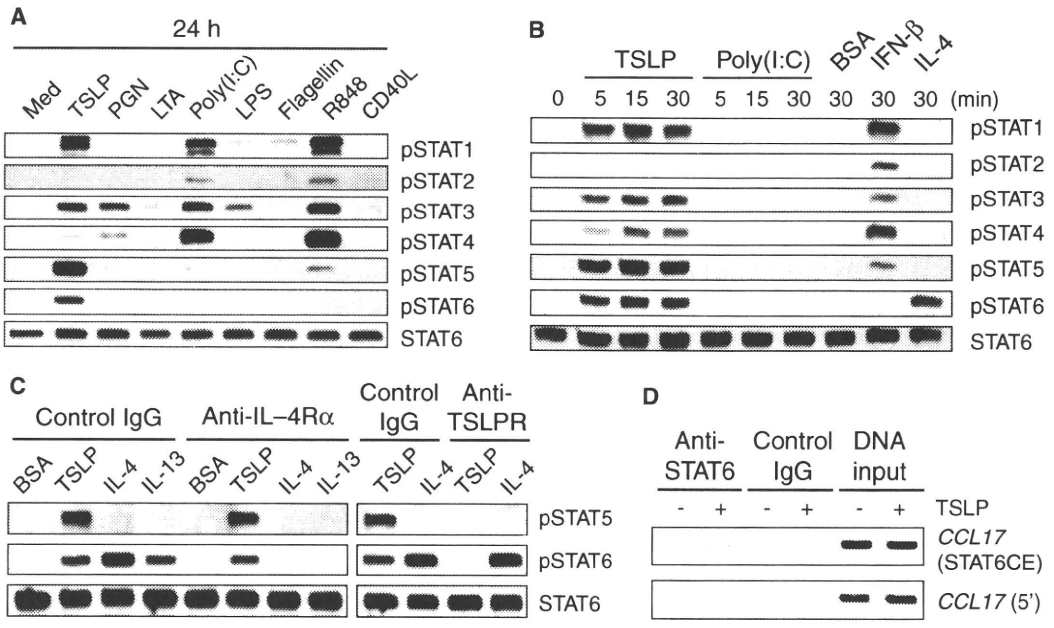

Fig. 1. TSLP directly activates STAT6 in mDCs. (**A**) Western blotting analysis was performed to compare the activation of different STAT proteins in mDCs cultured for 24 hours with medium alone (Med), TSLP (25 ng/ml), PGN, LTA, poly(I:C), LPS, flagellin, R848, or CD40L. (**B**) Western blotting analysis was performed to compare the early time course of activation of STAT proteins in mDCs stimulated with TSLP (25 ng/ml), poly(I:C), vehicle control (BSA), IFN-β (25 ng/ml), or IL-4 (25 ng/ml). (**C**) Effect of neutralizing antibodies against IL-4Rα or TSLPR on the activation of the indicated STAT proteins in mDCs by TSLP, IL-4, and IL-13. Cells were preincubated with the indicated neutralizing or isotype-matched control antibodies (10 μg/ml) for 30 min at 37°C and then stimulated with 10 ng/ml of TSLP, IL-4, or IL-13 or with vehicle control (BSA) for 10 min at 37°C. (A to C) Western blots were incubated with antibodies specific for the indicated phosphorylated STAT proteins or with an antibody against STAT6 to confirm equal loading of all lanes. Data are representative of three independent experiments. (**D**) ChIP assays demonstrating

dance of OX40L is the second unique feature of TSLP-mDCs. Because the promoter of *OX40L* contains two potential nuclear factor κB (NF-κB) binding sites (*25*) and because TSLP increases the expression of several NF-κB target genes in mDCs (fig. S4), we hypothesized that the NF-κB pathway might play a role in the increased production of OX40L that is triggered by TSLP but not by other stimuli (*12*). To delineate the differential activation of NF-κB by different stimuli, we compared the nuclear translocation of NF-κB molecules in mDCs cultured with medium alone, TSLP, poly(I:C), R848, or CD40L for 20 hours, when *OX40L* messenger RNA (mRNA) is undetectable, and for 42 hours, when *OX40L* mRNA is detectable (*12*) (Fig. 3A). TSLP induced a comparable nuclear translocation of the NF-κB molecules p52 and RelB to that induced by poly(I:C), R848, and CD40L at both time points. In addition, TSLP induced a robust nuclear translocation of p50 at both time points.

To determine whether the NF-κB components were capable of binding to the κB-like sequences of the *OX40L* promoter, we performed electrophoretic mobility shift assays (EMSAs) at 60 hours after treatment with TSLP, when the expression of *OX40L* and the production of OX40L protein reach maximal levels (*12*). TSLP and poly(I:C) induced distinct patterns of nuclear protein complexes bound to the κB-like sequences of the *OX40L* promoter, whereas they induced an identical pattern of nuclear protein complexes bound to the control probe containing the NF-Y binding site (Fig. 3B). Supershift assays demonstrated that the protein complexes bound to the κB-like sequences of the *OX40L* promoter observed in TSLP-mDCs contained predominantly p50 and, to a lesser extent, RelB and c-Rel (Fig. 3C). The findings that TSLP did not induce the accumulation of detectable amounts of nuclear c-Rel in mDCs (Fig. 3A) and that RelA was not detected in the protein complexes bound to the κB-like sequences of the *OX40L* promoter (Fig. 3C) suggest that p50 and RelB may be responsible for the activation of the *OX40L* promoter in TSLP-mDCs.

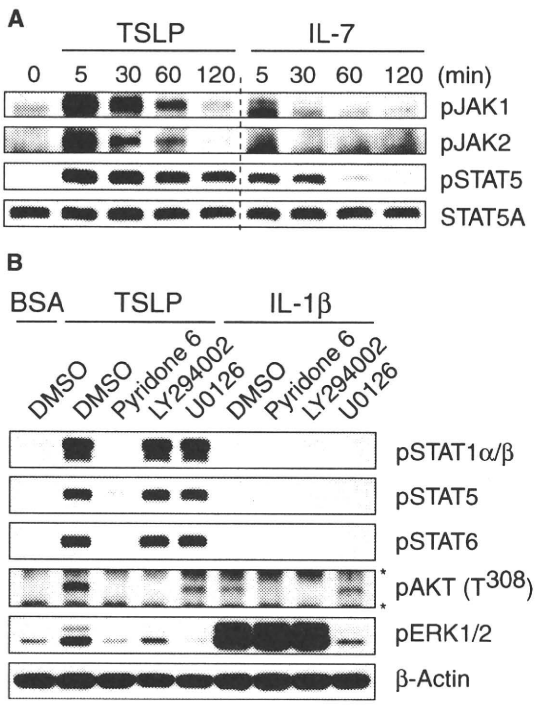

Fig. 2. Strong activation of JAK mediates sustained and broad TSLP-dependent signaling. (**A**) Western blotting analysis was performed to compare the kinetics of TSLP- and IL-7–mediated phosphorylation of JAK1, JAK2, and STAT5 in mDCs. Western blots were incubated with specific antibodies against the indicated phosphorylated proteins or with an antibody against STAT5A to confirm equal loading of all lanes. (**B**) Western blotting analysis was performed to demonstrate the contributions of JAK, PI3K, and ERK to TSLP-mediated signals. mDCs were pretreated with the pan-JAK inhibitor pyridone 6, the PI3K inhibitor LY294002, the MEK (ERK) inhibitor U0126, or DMSO (0.1%) for 30 min at 37°C and then were stimulated with 10 ng/ml of TSLP or IL-1β or with BSA for 10 min at 37°C. (*) Nonspecific bands. (A and B) The data shown are representative of three independent experiments.

To demonstrate the physiological binding of RelB to the *OX40L* promoter, we performed ChIP assays in primary human mDCs cultured with TSLP. The recruitment of RelB to the κB-like sequences of the *OX40L* promoter (Fig. 3D) was detected at 12 hours and was further increased in intensity at 48 hours (Fig. 3E and fig. S5). No substantial recruitment of RelA was detected. As a control, we observed that TSLP induced weak and transient binding of RelA (~24 hours) but stronger and more sustained binding of RelB (>48 hours) to the classical NF-κB binding site within the *CD40* promoter (*26*). To test whether p50 and RelB could activate the *OX40L* promoter, we performed luciferase reporter gene assays in human embryonic kidney (HEK) 293T cells. RelB, p50, or p52 alone did not activate the *OX40L* promoter, whereas RelB and p50, and to a lesser extent RelB and p52, did (Fig. 3F). Because p52 was not detected among the protein complexes that bound to the *OX40L* promoter (Fig. 3C), these data indicate that TSLP induced the nuclear translocation of p50, which formed a transcriptionally active complex with RelB to induce the expression of *OX40L* in mDCs.

Failure of TSLP to stimulate the production of IRF-8 and STAT4 underlies the uncoupling of DC maturation from IL-12 production

The third important feature that distinguishes TSLP-mDCs from TLR-activated DCs is that maturation of TSLP-DCs is uncoupled from the production of IL-12, an essential cytokine required for induction of T_H1 immune responses (*9*, *12*). Activation of PI3K-Akt and ERK pathways inhibits the production of IL-12 in DCs (*27*, *28*); however, poly(I:C)-induced production of IL-12 could not be dampened by concurrent stimulation with TSLP, which suggested that TSLP did not use dominant-negative regulators to inhibit the production of IL-12 (fig. S6). We therefore examined the potential roles of two stimulators of the production of IL-12, interferon regulatory factor 8 (IRF-8) (*29*, *30*), and STAT4 (*31*). Whereas TSLP did not increase the abundance of IRF-8 in mDCs, poly(I:C), R848, lipopolysaccharide (LPS), and CD40L did (Fig. 4A). TSLP weakly induced an increase in the abundance of STAT4 and a subtle change in the extent of STAT4 phosphorylation, whereas poly(I:C) and R848 strongly induced increases in both the abundance of STAT4 and the extent of its phosphorylation (Figs. 1, A and B, and 4B).

To directly demonstrate the role of IRF-8 and STAT4 in the production of IL-12 in human mDCs, IRF-8, STAT4, and, as a positive control, the adaptor protein myeloid differentiation marker 88 (MyD88) (*32*) were knocked down in human primary mDCs by small interfering RNAs (siRNAs) (Fig. 4C), and we examined the poly(I:C)-dependent production of IL-12 and the increased abundance of cell-surface CD86 in these cells. Reducing the abundance of IRF-8, STAT4, or MyD88 strongly suppressed poly(I:C)-induced production of IL-12p70 without affecting the increase in the abundance of CD86 (Fig. 4D), as was previously suggested in other cell types (*29*–*32*). These data demonstrate that the production of IL-12 can be uncoupled from DC maturation (as assessed by the increased abundance of CD86) and that IRF-8 and STAT4 mediate the production of IL-12 but not the maturation of DCs. The inability of TSLP to increase the abundance

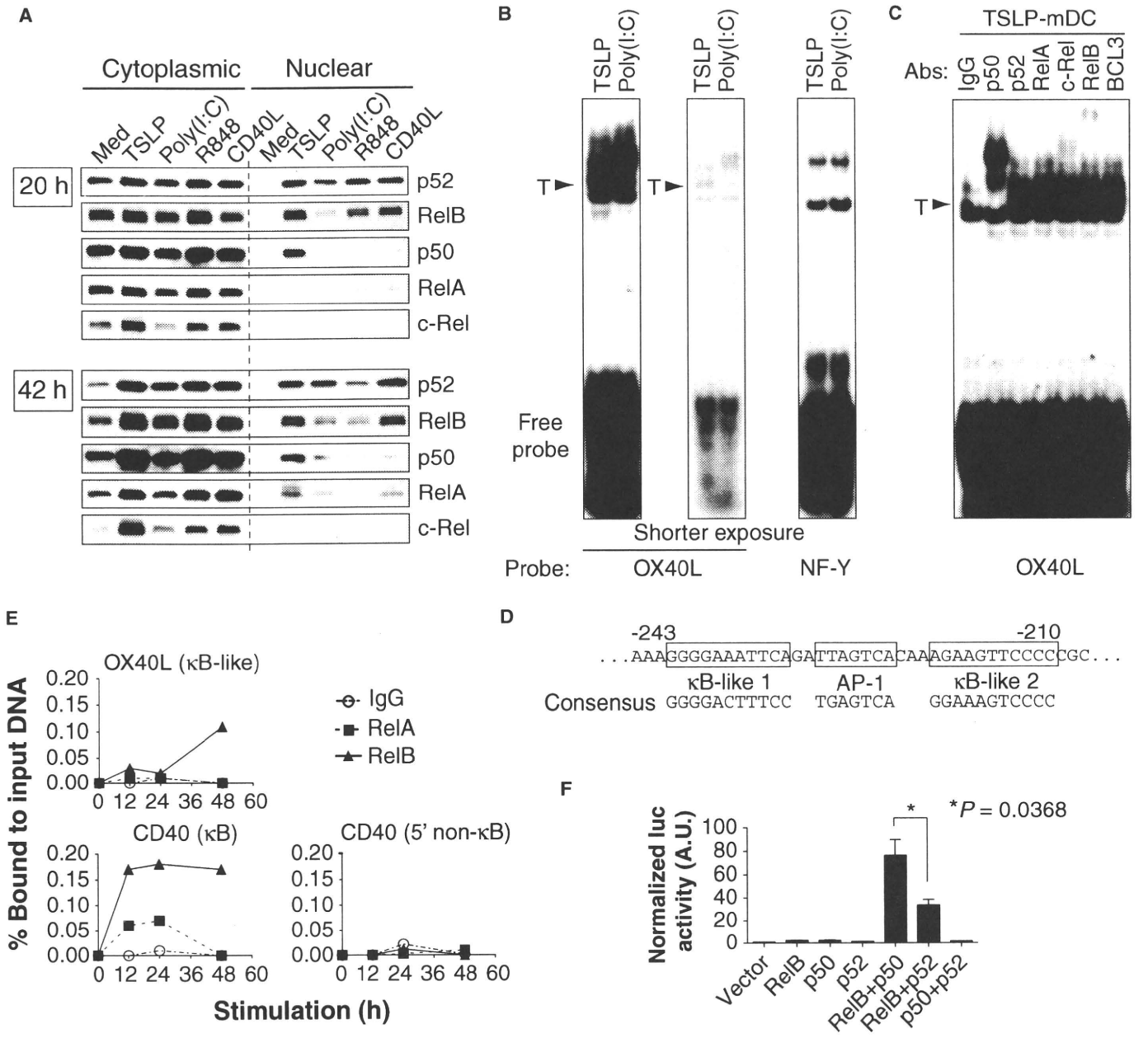

Fig. 3. TSLP activates NF-κB–dependent pathways that lead to the increased abundance of OX40L at the cell surface of mDCs. (**A**) Western blotting analysis was performed to demonstrate the cytoplasmic and nuclear localization of NF-κB molecules in mDCs 20 and 42 hours after culture with medium alone (Med), TSLP, poly(I:C), R848, or CD40L. (**B**) EMSA showing the binding of nuclear proteins to probes for the κB-like sequence of the promoter of *OX40L* and the binding sequence of the "housekeeping" transcription factor NF-Y in mDCs cultured for 60 hours with TSLP or poly(I:C). For the experiment with the *OX40L* probe, an autoradiograph of the same gel after a shorter exposure time is added to show the band separation. T, TSLP-predominant bands. (**C**) Supershift assays were performed with antibodies against the indicated NF-κB molecules and BCL3 to demonstrate the composition of the nuclear proteins bound to the κB-like sequence probe of *OX40L* from mDCs cultured for 60 hours with TSLP. (**D**) Nucleotide sequence of the region surrounding the potential NF-κB binding sites within the 5′-flanking region of *OX40L*. The nucleotide positions indicate the relative distance from the initiator codon. The sequences of the consensus κB site and the activating protein 1 (AP-1) site are depicted. (**E**) ChIP assays demonstrating the kinetics of the recruitment of RelA and RelB to the promoters of *OX40L* and *CD40* in TSLP-treated mDCs. Data are expressed as the percentage binding of either protein to the input DNA amount by quantifying the intensities of PCR-amplified bands. (A to C, and E) Data are representative of three independent experiments. (**F**) NF-κB–dependent activation of the *OX40L* promoter in HEK 293T cells was determined by luciferase reporter assay. Error bars represent the SEM from three independent experiments.

of IRF-8 and STAT4 in human primary mDCs (Fig. 4, A and B) may therefore explain the absence of IL-12 production by TSLP-mDCs.

DISCUSSION

Here, we demonstrated that TSLP induces a unique compound signal that programs mDCs to induce T_H2 responses that is distinct from those signals induced by other known activators of mDCs such as poly(I:C), R848, LPS, peptidoglycan (PGN), and CD40L, which normally activate mDCs to induce T_H1-type responses. In experiments with human primary mDCs we found that TSLP induced broad and robust JAK-dependent signaling. In particular, TSLP directly activated STAT6, which explains the unique ability of TSLP-mDCs to produce the T_H2-attracting chemokine CCL17. Previous studies on TSLP signaling with TSLPR-expressing cell lines failed to detect the activation of JAKs and STAT6, which underscores the importance of analyzing primary cells. The human mDCs used in this study are in vivo–derived mDCs that represent about 0.5% of total peripheral blood mononuclear cells. We did not use mDCs generated in vitro from blood monocytes or from $CD34^+$ hematopoietic progenitor cells because they do not respond to TSLP (*33*). The yield of mDCs per buffy coat sample (which represents about 500 ml of human peripheral blood) is about 500,000 cells. For typical experiments, we used 2×10^6 to 5×10^6 mDCs (at >99% purity) that were isolated by cell sorting of 4 to 10 human blood buffy coat samples. Our study thus shows the feasibility of conducting comprehensive cell signaling studies in rare primary human DCs.

The second most important feature of TSLP signaling in human primary mDCs is that it increases the abundance at the cell surface of OX40L, a key molecule for polarizing naïve $CD4^+$ T cell differentiation into inflammatory T_H2 cells through the activation of the NF-κB pathway. Notably, TSLP-induced nuclear p50 and RelB to contribute to the expression of *OX40L* in mDCs (*12*, *13*). However, *OX40L* is distinct from many of the typical NF-κB–regulated genes, such as those that encode MHC II and the costimulatory molecules CD40, CD80, and CD86, whose promoter regions contain the well-conserved consensus NF-κB binding sites (κB sites). The *OX40L* promoter, on the other hand, contains two atypical NF-κB binding sites that consist of 11 base pairs (bp) (κB-like sequences; Fig. 3D), which may have relatively low binding affinity for canonical NF-κB dimers (*25*). It was postulated that the p50 homodimer preferably recognizes an 11-bp DNA sequence, whereas the RelA homodimer and the RelA-p50 heterodimer prefer 9- and 10-bp DNA sequences, respectively (*34*). This unique feature of the *OX40L* promoter region may explain (i) why TSLP, but not other stimuli such as poly(I:C) and CD40L, efficiently induces the expression of *OX40L*, and (ii) why it takes 48 to 72 hours for TSLP to induce the expression of *OX40L* as opposed to its faster (~24-hour) induction of the expression of the genes encoding MHC II, CD40, CD80, and CD86 in mDCs. Our study also suggests that the type of nuclear NF-κB components or complexes may dictate the ability to activate the *OX40L* promoter in mDCs. The nuclear p50-RelB complex induced by TSLP is relatively more efficient in binding to the two atypical κB-like sequences in the *OX40L* promoter and therefore in activating the expression of *OX40L* than are the typical NF-κB complexes. During immune responses to pathogens, the production of different costimulatory and coinhibitory molecules on APCs have different kinetics (*35*). Our study suggests that the nature of the NF-κB binding sites within the promoter regions of the genes that encode these molecules may represent "molecular timers" of their expression.

The third important feature of TSLP signaling in human primary mDCs is that TSLP does not increase the abundance of IRF-8 or STAT4, the two critical transcription factors required for the production of IL-12 in mDCs. The maturation of mDCs by various TLR ligands and CD40L is coupled with the production of IL-12 by the DCs (*4*–*8*). However, maturation of mDCs induced by TSLP, including the increased abundance of MHC II, CD40, CD80, and CD86, is uncoupled from the production of IL-12 (*9*, *12*). Given that the activation of NF-κB is a critical signal for DC maturation (*36*), our study suggests that the uncoupling of mDC maturation from the production of IL-12 is due to the ability of TSLP to activate multiple NF-κB components without the apparent induction of the expression of *IRF-8* or *STAT4*. Because the activation of NF-κB is involved in the TLR- or CD40L-mediated expression of *STAT4* in monocyte-derived DCs (*37*), TSLP-mediated activation of NF-κB may be qualitatively different from that induced by TLR ligands or CD40L.

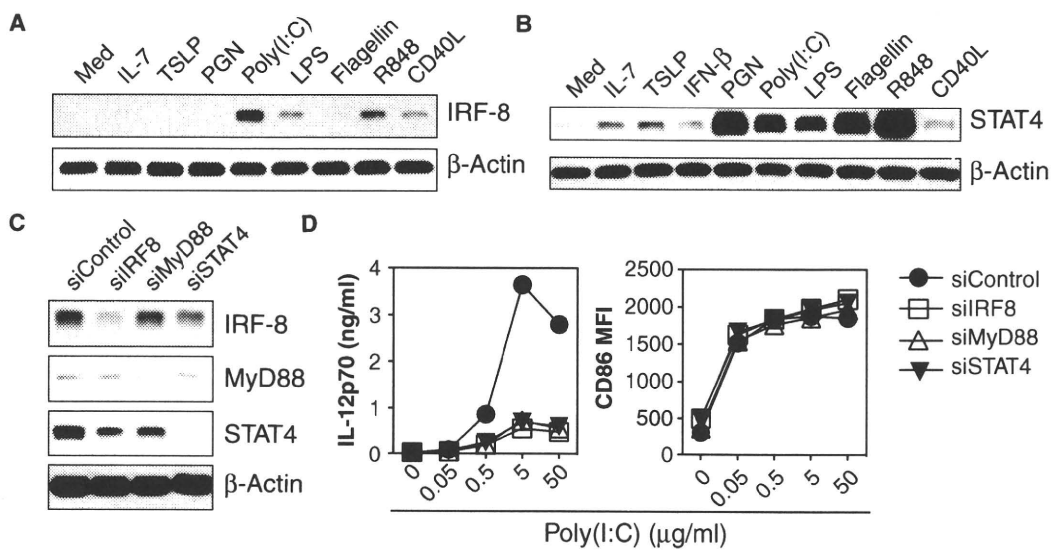

Fig. 4. TSLP does not stimulate the production of IRF-8 or STAT4, essential factors for the production of IL-12 by mDCs. (**A**) Western blotting analysis was performed to compare the differential regulation of the abundance of IRF-8 in mDCs that were activated for 24 hours by the indicated stimuli, as described in Fig. 1A with the inclusion of IL-7 (25 ng/ml) and the exclusion of LTA. (**B**) Western blotting analysis was performed to compare the abundance of STAT4 in mDCs after 24 hours of activation by the indicated stimuli, as described in (A) with the inclusion of IFN-β (25 ng/ml). (**C**) Western blotting analysis was performed to show the efficiency of knockdown of the indicated proteins in poly(I:C) (5 μg/ml)-stimulated mDCs transfected with siRNAs specific for IRF-8, MyD88, or STAT4 or with a nontargeting control siRNA (siControl). (A to C) Western blots were incubated with antibody against β-actin to demonstrate equivalent loading of all lanes. (**D**) siRNA-transfected mDCs were stimulated with poly(I:C) for 24 hours and the concentration of IL-12p70 in the culture supernatants and the mean fluorescent intensity (MFI) of cell-surface CD86 are depicted. Data are representative of three (A and B) or five (C and D) independent experiments.

In conclusion, this study demonstrates that TSLP programs human mDCs to induce T_H2 responses by activating multiple signal pathways in a unique manner. The functional plasticity of mDCs to induce distinct T helper cell responses relies on elaborate signal codes generated by the activation of different receptors on mDCs. This study also highlights the importance and the feasibility of studying signal transduction in rare human primary cells.

MATERIALS AND METHODS

Reagents

PGN from *Bacillus subtilis* (5 μg/ml); lipoteichoic acid (LTA, 1 μg/ml), poly(I:C) (25 μg/ml, unless otherwise stated), LPS from *Escherichia coli* O111:B4 (1 μg/ml), flagellin from *Salmonella typhimurium* (5 μg/ml), and R848 (1 μg/ml) were purchased from InvivoGen. Recombinant human IL-2 and IFN-β were purchased from PeproTech. Recombinant human IL-1β, IL-4, IL-7, and neutralizing antibodies against IL-4Rα were purchased from R&D Systems. Recombinant human TSLP was either purchased from R&D Systems or expressed in HEK 293A cells and purified as described previously (*12*). These two independent recombinant TSLP proteins exhibited identical signal transduction capabilities. All recombinant cytokines were resuspended in phosphate-buffered saline containing 0.1% BSA, which was used as a vehicle control, where applicable. Neutralizing mouse antibodies against TSLPR (clone 1F11) were developed in our laboratory. Recombinant soluble CD40L (1 μg/ml) and Enhancer Solution (1 μg/ml) (Alexis Biochemicals) were used to stimulate CD40. The pan-JAK inhibitor pyridone 6 (*38*) (16 μM for the treatment of DCs), the PI3K inhibitor LY294002 (32.5 μM), and the MEK (ERK) inhibitor U0126 (10 μM) were purchased from EMD Biosciences and dissolved in DMSO before use.

Purification and culture of mDCs

The Institutional Review Board (IRB) for Human Research at The University of Texas M. D. Anderson Cancer Center approved this study. $CD11c^+lineage^-$ mDCs were isolated from the blood of healthy donors with a FACSAria (BD Biosciences) as previously described (*12*). Sorted $CD11c^+$ mDCs with purity >99% were cultured in RPMI 1640 medium (Invitrogen) containing 5% fetal calf serum (FCS) (Atlanta Biologicals). For short-term stimulation, freshly isolated mDCs were cultured in medium alone for 18 hours before stimulation.

Western blotting analysis

Cultured mDCs were collected and lysed with the PhosphoSafe Extraction Buffer (EMD Biosciences) supplemented with proteinase inhibitors [1 mM Pefabloc, 10 μM leupeptin, and 5 mM EDTA (Thermo Fisher Scientific)] for 10 min at room temperature. In some experiments, cytoplasmic and nuclear proteins were separated with the NE/PER Nuclear and Cytoplasmic Extraction Reagents (Thermo Fisher Scientific). Cell lysates were mixed with SDS sample buffer and boiled for 5 min. Samples were subjected to Western blotting analysis with antibodies against phosphorylated STAT1 (pSTAT1) (Tyr^{701}), pSTAT2 (Tyr^{690}), pSTAT3 (3E2) (Tyr^{705}), pSTAT5 (Tyr^{694}), pSTAT6 (Tyr^{641}), STAT4 (C46B10), pJak1 ($Tyr^{1022/1023}$), pAkt (Thr^{308}), Akt (5G3), pERK1/2, pp38 MAPK, inhibitor of NF-κBα (IκBα; Cell Signaling Technology); pSTAT4 (Tyr^{693}) (BD Biosciences); STAT1 (E-23), STAT3 (C-20), STAT6 (S-20 or M-20), pJak2 ($Tyr^{1007/1008}$), p50 (E-10), RelA (C-20), RelB (C-19), c-Rel (N), IRF-4 (N-18), IRF-8 (C-19), BCL3 (C-14) (Santa Cruz Biotechnology); p52 (#05-361) (Millipore); active JNK (Promega); STAT5A (R&D Systems); MyD88 (Invitrogen); or β-actin (Sigma-Aldrich). To detect different proteins on the same membrane, bound antibodies were stripped off by incubating the membrane in either the Restore PLUS Western Blot Stripping Buffer (Thermo Fisher Scientific) or 62.5 mM tris-HCl (pH 6.5), 2% SDS, 0.68% (v/v) β-mercaptoethanol for 5 min at room temperature, or 30 min at 55°C, respectively, and then intensive washing.

ChIP assays

ChIP assays were performed with the ChIP assay kit (Millipore) with slight modifications to the manufacturer's instructions. To detect the binding of STAT6 to DNA, we used 0.4% formaldehyde for cross-linking as reported (*17*). To detect the binding of RelA or RelB to DNA, we conducted a two-step cross-linking method as previously reported (*39*). Antibodies against STAT6 (M-20), RelA (C-20), and RelB (C-19) (Santa Cruz Biotechnology) were used for the immunoprecipitations. Primers for the detection of precipitated DNA by polymerase chain reaction (PCR) assay were as follows: *CCL17* (TARC), surrounding region of STAT6 binding site, 5′-CAG CTG TGC GTG GAG GCT TTT CA-3′ and 5′-TCC TTC CCT AGA CCA GTG AAG TTC GAA GA-3′; 6000-bp upstream region, 5′-ACA AGT GGG CAG AGA GGA AA-3′ and 5′-TCA GTT GCA CTG CCA TCT TC-3′); *TNFSF4* (OX40L), surrounding region of κB-like sequences, 5′-CCT GTT AGC CCA GAG GAA AA-3′ and 5′-CCA GGG CCA GAG ATA AAA GG-3′); and *TNFRSF5* (CD40) (*26*), surrounding region of proximal κB site, 5′-GAG GTG GGA TGG AAT GGA AT-3′ and 5′-GTA TGG GGA GGC GTT TCA AG-3′; 2500-bp upstream non-κB region, 5′-TTG CTG AAC CCA CTC ATT CA-3′ and 5′-AGC ATT TAG CAT GCC AGC TC-3′.

EMSAs

Nuclear extracts were subjected to EMSAs with a ^{32}P-radiolabeled *OX40L* promoter κB-like sequence oligonucleotide probe (5′-AAA GGG GAA ATT CAG ATT AGT CAC AAA GAA GTT CCC CCG-3′) or a control probe bound by the constitutive transcription factor NF-Y (5′-AAA AGA TTA ACC AAT CAC GTA CGG TCT-3′). Antibodies against p50 (NLS), p52 (C-5), RelA (A), c-Rel (N), RelB (C-19), and BCL3 (C-14) (Santa Cruz Biotechnology) were used for supershift assays.

Luciferase reporter assays

All plasmids were constructed by standard molecular biology techniques. HEK 293T cells were maintained in Dulbecco's modified Eagle's medium (Invitrogen) supplemented with 10% FCS. Cells were transiently transfected with a 1000-bp *OX40L* promoter-inserted firefly luciferase reporter plasmid (pGL-4.10, Promega), a constitutive *Renilla* luciferase expression vector phRL-TK (Promega), and expression vectors for NF-κB molecules (RelB, p50, and p52) by Lipofectamine 2000 (Invitrogen) according to the manufacturer's instructions. Promoter activity was measured with the DLR kit (Promega) on a Sirius luminometer (Berthold Detection Systems) and expressed as arbitrary units (firefly luciferase activity normalized by *Renilla* luciferase activity). Statistical analysis was performed with the two-tailed Student's *t* test with Prism software (GraphPad).

Transfection of mDCs with siRNAs

Freshly isolated mDCs were precultured with granulocyte-macrophage colony-stimulating factor (GM-CSF, R&D Systems, 50 ng/ml) for 18 hours, and cells were transfected with siRNAs at a final concentration of 120 nM with Lipofectamine 2000-CD (Invitrogen) according to the manufacturer's instructions. One day after transfection, cells were resuspended in fresh medium and stimulated with poly(I:C) for 24 hours. The following Dharmacon ON-TARGETplus SMARTpool siRNA reagents (Thermo Fisher Scientific) were used: IRF-8 (Dharmacon Catalog # L-011699-00), STAT4 (L-011784-00), MYD88 (L-004769-00), and Non-targeting pool (D-001810-10).

ELISAs

The amount of human IL-12p70 in culture supernatants was measured by DuoSet ELISA development kit (R&D Systems) according to the manufacturer's instructions.

Flow cytometry

The abundance of CD86 on the surface of mDCs was analyzed by a FACSCalibur with a fluorescein isothiocyanate–conjugated antibody against CD86 (BD Biosciences), and the geometric means of the fluorescent signals were used to express the results in terms of mean fluorescence intensity (MFI).

SUPPLEMENTARY MATERIALS

www.sciencesignaling.org/cgi/content/full/3/105/ra4/DC1

Fig. S1. R848 is a weaker inducer of STAT5 phosphorylation than is TSLP.

Fig. S2. TSLP, but not IL-7 or IL-4, is capable of inducing the activation of a range of STAT proteins in mDCs.

Fig. S3. TSLP induces the phosphorylation of ERK, JNK, and Akt in mDCs.

Fig. S4. TSLP increases the abundance of NF-κB target molecules in mDCs.

Fig. S5. PCR gel electrophoresis data for the ChIP assays shown in Fig. 3E.

Fig. S6. TSLP is not a dominant-negative regulator of the production of IL-12.

REFERENCES AND NOTES

1. J. Banchereau, F. Briere, C. Caux, J. Davoust, S. Lebecque, Y.-J. Liu, B. Pulendran, K. Palucka, Immunobiology of dendritic cells. *Annu. Rev. Immunol.* **18**, 767–811 (2000).
2. S. E. Macatonia, N. A. Hosken, M. Litton, P. Vieira, C. S. Hsieh, J. A. Culpepper, M. Wysocka, G. Trinchieri, K. M. Murphy, A. O'Garra, Dendritic cells produce IL-12 and direct the development of Th1 cells from naive $CD4^+$ T cells. *J. Immunol.* **154**, 5071–5079 (1995).
3. M. Cella, D. Scheidegger, K. Palmer-Lehmann, P. Lane, A. Lanzavecchia, G. Alber, Ligation of CD40 on dendritic cells triggers production of high levels of interleukin-12 and enhances T cell stimulatory capacity: T-T help via APC activation. *J. Exp. Med.* **184**, 747–752 (1996).
4. P. Kaliński, C. M. Hilkens, E. A. Wierenga, M. L. Kapsenberg, T-cell priming by type-1 and type-2 polarized dendritic cells: The concept of a third signal. *Immunol. Today* **20**, 561–567 (1999).
5. M. Moser, K. M. Murphy, Dendritic cell regulation of T_H1-T_H2 development. *Nat. Immunol.* **1**, 199–205 (2000).
6. B. Pulendran, K. Palucka, J. Banchereau, Sensing pathogens and tuning immune responses. *Science* **293**, 253–256 (2001).
7. A. Lanzavecchia, F. Sallusto, The instructive role of dendritic cells on T cell responses: Lineages, plasticity and kinetics. *Curr. Opin. Immunol.* **13**, 291–298 (2001).
8. A. Boonstra, C. Asselin-Paturel, M. Gilliet, C. Crain, G. Trinchieri, Y.-J. Liu, A. O'Garra, Flexibility of mouse classical and plasmacytoid-derived dendritic cells in directing T helper type 1 and 2 cell development: Dependency on antigen dose and differential Toll-like receptor ligation. *J. Exp. Med.* **197**, 101–109 (2003).
9. V. Soumelis, P. A. Reche, H. Kanzler, W. Yuan, G. Edward, B. Homey, M. Gilliet, S. Ho, S. Antonenko, A. Lauerma, K. Smith, D. Gorman, S. Zurawski, J. Abrams, S. Menon, T. McClanahan, R. de Waal-Malefyt, F. Bazan, R. A. Kastelein, Y.-J. Liu, Human epithelial cells trigger dendritic cell mediated allergic inflammation by producing TSLP. *Nat. Immunol.* **3**, 673–680 (2002).
10. A. Al-Shami, R. Spolski, J. Kelly, A. Keane-Myers, W. J. Leonard, A role for TSLP in the development of inflammation in an asthma model. *J. Exp. Med.* **202**, 829–839 (2005).
11. B. Zhou, M. R. Comeau, T. De Smedt, H. D. Liggitt, M. E. Dahl, D. B. Lewis, D. Gyarmati, T. Aye, D. J. Campbell, S. F. Ziegler, Thymic stromal lymphopoietin as a key initiator of allergic airway inflammation in mice. *Nat. Immunol.* **6**, 1047–1053 (2005).
12. T. Ito, Y. H. Wang, O. Duramad, T. Hori, G. J. Delespesse, N. Watanabe, F. X. Qin, Z. Yao, W. Cao, Y.-J. Liu, TSLP-activated dendritic cells induce an inflammatory T helper type 2 cell response through OX40 ligand. *J. Exp. Med.* **202**, 1213–1223 (2005).
13. D. Seshasayee, W. P. Lee, M. Zhou, J. Shu, E. Suto, J. Zhang, L. Diehl, C. D. Austin, Y. G. Meng, M. Tan, S. L. Bullens, S. Seeber, M. E. Fuentes, A. F. Labrijn, Y. M. Graus, L. A. Miller, E. S. Schelegle, D. M. Hyde, L. C. Wu, S. G. Hymowitz, F. Martin, In vivo blockade of OX40 ligand inhibits thymic stromal lymphopoietin driven atopic inflammation. *J. Clin. Invest.* **117**, 3868–3878 (2007).
14. Y.-J. Liu, V. Soumelis, N. Watanabe, T. Ito, Y. H. Wang, R. de Waal Malefyt, M. Omori, B. Zhou, S. F. Ziegler, TSLP: An epithelial cell cytokine that regulates T cell differentiation by conditioning dendritic cell maturation. *Annu. Rev. Immunol.* **25**, 193–219 (2007).
15. S. D. Levin, R. M. Koelling, S. L. Friend, D. E. Isaksen, S. F. Ziegler, R. M. Perlmutter, A. G. Farr, Thymic stromal lymphopoietin: A cytokine that promotes the development of IgM^+ B cells in vitro and signals via a novel mechanism. *J. Immunol.* **162**, 677–683 (1999).
16. P. A. Reche, V. Soumelis, D. M. Gorman, T. Clifford, M. Liu, M. Travis, S. M. Zurawski, J. Johnston, Y. J. Liu, H. Spits, R. de Waal Malefyt, R. A. Kastelein, J. F. Bazan, Human thymic stromal lymphopoietin preferentially stimulates myeloid cells. *J. Immunol.* **167**, 336–343 (2001).
17. G. Wirnsberger, D. Hebenstreit, G. Posselt, J. Horejs-Hoeck, A. Duschl, IL-4 induces expression of TARC/CCL17 via two STAT6 binding sites. *Eur. J. Immunol.* **36**, 1882–1891 (2006).
18. K. Liddiard, J. S. Welch, J. Lozach, S. Heinz, C. K. Glass, D. R. Greaves, Interleukin-4 induction of the CC chemokine TARC (CCL17) in murine macrophages is mediated by multiple STAT6 sites in the TARC gene promoter. *BMC Mol. Biol.* **7**, 45 (2006).
19. J. Zhu, J. Cote-Sierra, L. Guo, W. E. Paul, Stat5 activation plays a critical role in Th2 differentiation. *Immunity* **19**, 739–748 (2003).
20. T. Ito, H. Kanzler, O. Duramad, W. Cao, Y.-J. Liu, Specialization, kinetics, and repertoire of type 1 interferon responses by human plasmacytoid predendritic cells. *Blood* **107**, 2423–2431 (2006).
21. G. Gautier, M. Humbert, F. Deauvieau, M. Scuiller, J. Hiscott, E. E. Bates, G. Trinchieri, C. Caux, P. Garrone, A type I interferon autocrine–paracrine loop is involved in Toll-like receptor-induced interleukin-12p70 secretion by dendritic cells. *J. Exp. Med.* **201**, 1435–1446 (2005).
22. W. J. Leonard, J. J. O'Shea, Jaks and STATs: Biological implications. *Annu. Rev. Immunol.* **16**, 293–322 (1998).
23. D. Hebenstreit, G. Wirnsberger, J. Horejs-Hoeck, A. Duschl, Signaling mechanisms, interaction partners, and target genes of STAT6. *Cytokine Growth Factor Rev.* **17**, 173–188 (2006).
24. J. N. Ihle, Cytokine receptor signalling. *Nature* **377**, 591–594 (1995).
25. K. Ohtani, A. Tsujimoto, T. Tsukahara, N. Numata, S. Miura, K. Sugamura, M. Nakamura, Molecular mechanisms of promoter regulation of the gp34 gene that is trans-activated by an oncoprotein Tax of human T cell leukemia virus type I. *J. Biol. Chem.* **273**, 14119–14129 (1998).
26. M. Tone, Y. Tone, J. M. Babik, C. Y. Lin, H. Waldmann, The role of Sp1 and NF-κB in regulating CD40 gene expression. *J. Biol. Chem.* **277**, 8890–8897 (2002).
27. T. Fukao, M. Tanabe, Y. Terauchi, T. Ota, S. Matsuda, T. Asano, T. Kadowaki, T. Takeuchi, S. Koyasu, PI3K-mediated negative feedback regulation of IL-12 production in DCs. *Nat. Immunol.* **3**, 875–881 (2002).
28. S. Agrawal, A. Agrawal, B. Doughty, A. Gerwitz, J. Blenis, T. Van Dyke, B. Pulendran, Cutting edge: Different Toll-like receptor agonists instruct dendritic cells to induce distinct Th responses via differential modulation of extracellular signal-regulated kinase-mitogen-activated protein kinase and c-Fos. *J. Immunol.* **171**, 4984–4989 (2003).
29. N. A. Giese, L. Gabriele, T. M. Doherty, D. M. Klinman, L. Tadesse-Heath, C. Contursi, S. L. Epstein, H. C. Morse III, Interferon (IFN) consensus sequence-binding protein, a transcription factor of the IFN regulatory factor family, regulates immune responses in vivo through control of interleukin 12 expression. *J. Exp. Med.* **186**, 1535–1546 (1997).
30. T. Scharton-Kersten, C. Contursi, A. Masumi, A. Sher, K. Ozato, Interferon consensus sequence binding protein–deficient mice display impaired resistance to intracellular infection due to a primary defect in interleukin 12 p40 induction. *J. Exp. Med.* **186**, 1523–1534 (1997).
31. N. Tokumasa, A. Suto, S. Kagami, S. Furuta, K. Hirose, N. Watanabe, Y. Saito, K. Shimoda, I. Iwamoto, H. Nakajima, Expression of Tyk2 in dendritic cells is required for IL-12, IL-23, and IFN-γ production and the induction of Th1 cell differentiation. *Blood* **110**, 553–560 (2007).
32. L. Alexopoulou, A. C. Holt, R. Medzhitov, R. A. Flavell, Recognition of double-stranded RNA and activation of NF-κB by Toll-like receptor 3. *Nature* **413**, 732–738 (2001).
33. T. Akamatsu, N. Watanabe, M. Kido, K. Saga, J. Tanaka, K. Kuzushima, A. Nishio, T. Chiba, Human TSLP directly enhances expansion of $CD8^+$ T cells. *Clin. Exp. Immunol.* **154**, 98–106 (2008).
34. Y. Q. Chen, S. Ghosh, G. Ghosh, A novel DNA recognition mode by the NF-κB p65 homodimer. *Nat. Struct. Biol.* **5**, 67–73 (1998).
35. S. Wang, L. Chen, T lymphocyte co-signaling pathways of the B7-CD28 family. *Cell. Mol. Immunol.* **1**, 37–42 (2004).
36. M. Rescigno, M. Martino, C. L. Sutherland, M. R. Gold, P. Ricciardi-Castagnoli, Dendritic cell survival and maturation are regulated by different signaling pathways. *J. Exp. Med.* **188**, 2175–2180 (1998).
37. M. E. Remoli, J. Ragimbeau, E. Giacomini, V. Gafa, M. Severa, R. Lande, S. Pellegrini, E. M. Coccia, NF-κB is required for STAT-4 expression during dendritic cell maturation. *J. Leukoc. Biol.* **81**, 355–363 (2007).

38. J. E. Thompson, R. M. Cubbon, R. T. Cummings, L. S. Wicker, R. Frankshun, B. R. Cunningham, P. M. Cameron, P. T. Meinke, N. Liverton, Y. Weng, J. A. DeMartino, Photochemical preparation of a pyridone containing tetracycle: A Jak protein kinase inhibitor. *Bioorg. Med. Chem. Lett.* **12**, 1219–1223 (2002).
39. B. Tian, D. E. Nowak, M. Jamaluddin, S. Wang, A. R. Brasier, Identification of direct genomic targets downstream of the nuclear factor-κB transcription factor mediating tumor necrosis factor signaling. *J. Biol. Chem.* **280**, 17435–17448 (2005).
40. We thank S. S. Watowich for critical reading of the manuscript; M. J. Wentz for preparation of the manuscript; Y.-L. Li-Yuan, W. Cao, and Y.-H. Wang for helpful suggestions; and K. Ramirez and Z. He for assistance with cell sorting. Our cell sorting facility is supported by grant P30CA16672 from the National Cancer Institute. Y.-J.L. is supported by M. D. Anderson Cancer Center Foundation and the National Institute of Allergy and Infectious Diseases (grants AI061645 and U19 AI071130).

Submitted 4 August 2009
Accepted 28 December 2009
Final Publication 19 January 2010
10.1126/scisignal.2000567
Citation: K. Arima, N. Watanabe, S. Hanabuchi, M. Chang, S.-C. Sun, Y.-J. Liu, Distinct signal codes generate dendritic cell functional plasticity. *Sci. Signal.* **3**, ra4 (2010).